Galindez-Najera, Silvia P, Choomjaihan, Prasan, Barron, Cecile, Lullien-Pellerin, Valerie and Campbell, Grant M.

A compositional breakage equation for wheat milling

Accepted Manuscript

A compositional breakage equation for wheat milling

S.P. Galindez-Najera, P. Choomjaihan, C. Barron, V. Lullien-Pellerin, G.M. Campbell

PII: S0260-8774(16)30060-7

DOI: 10.1016/j.jfoodeng.2016.03.001

Reference: JFOE 8499

To appear in: *Journal of Food Engineering*

Received Date: 16 November 2015

Revised Date: 1 March 2016

Accepted Date: 2 March 2016

Please cite this article as: Galindez-Najera, S., Choomjaihan, P, Barron, C, Lullien-Pellerin, V, Campbell, G., A compositional breakage equation for wheat milling, *Journal of Food Engineering* (2016), doi: 10.1016/j.jfoodeng.2016.03.001.

A compositional breakage equation for wheat milling

Galindez-Najera SP[1], Choomjaihan P[2], Barron C[3], Lullien-Pellerin V[3] and Campbell GM[1,4*]

1. Satake Centre for Grain Process Engineering, School of Chemical Engineering and Analytical Science, The University of Manchester, Oxford Rd, Manchester, M13 9PL, UK
2. Curriculum of Agricultural Engineering, Department of Mechanical Engineering, Faculty of Engineering, King Mongkut's Institute of Technology Ladkrabang, Bangkok, 10520, Thailand
3. UMR 1208 Ingénierie des Agropolymères et Technologies Emergentes, INRA, UMII, Cirad, Montpellier Supagro 2, Place P. Viala, bâtiment 31, 34060 Montpellier Cedex 2, France
4. Current address: School of Applied Sciences, University of Huddersfield, Queensgate, Huddersfield, HD1 3DH, UK
* corresponding author: g.campbell@hud.ac.uk

Abstract

The compositional breakage equation is derived, in which the distributions of botanical components following milling of wheat are defined in terms of compositional breakage functions and concentration functions. The forms of the underlying functions are determined using experimental data for Outer Pericarp, Intermediate Layer, Aleurone and Starchy Endosperm generated from spectroscopic analysis of milled fractions of a hard and a soft wheat milled under Sharp-to-Sharp (S-S) and Dull-to-Dull (D-D) dispositions. For the hard Mallacca wheat, the Outer Pericarp, Intermediate Layer and Aleurone compositions mostly varied with particle size in similar ways, consistent with these layers fusing together as "bran" and breaking together, although with possibly a subtle difference around the production of very fine particles under D-D milling. By contrast, for the soft Consort wheat, Outer Pericarp, Intermediate Layer and Aleurone were distributed in broken particles very differently, particularly under D-D milling, suggesting a different breakage mechanism associated with differences in the mechanical properties and adhesion of the bran layers. These new insights into the nature of wheat breakage and the contributions of the component tissues could have implications for wheat breeding and flour mill operation.

Keywords

flour milling; composition; pericarp; aleurone; endosperm; breakage function

Introduction

In the 1950s Broadbent and Callcott introduced breakage matrices to relate input and output particle size distributions during grinding operations (Broadbent and Callcott, 1956a, 1956b, 1957). They used square matrices in which the input and output particle size distributions covered the same size ranges, and applied this approach to model coal grinding. Campbell and Webb (2001) applied the breakage matrix approach to roller milling of wheat, extending the approach to use non-square matrices covering different size ranges for the input and output particle size distributions, thus improving the applicability and accuracy of the approach.

A complete understanding of milling requires the ability to predict the size distribution of broken particles and also the composition of particles of different sizes. Fistes and Tanovic (2006) demonstrated that compositional breakage matrices could also be constructed that, combined with breakage matrices for predicting output particle size, allowed the composition of those output particles also to be predicted. They also employed roller milling of wheat as the system with which to demonstrate the value of predictions for composition as well as size; the key feature of roller milling of wheat is that the bran tends to stay as large particles and the endosperm as small particles, hence facilitating separation of bran and endosperm by sifting.

Subsequent work by Campbell and co-workers focussed on the continuous form of the breakage equation and of breakage functions, rather than the discrete forms that underpin the construction of breakage matrices; continuous functions are more generally applicable and more readily interpretable, thus yielding greater predictive power and greater mechanistic insights regarding wheat breakage. This body of work has allowed the effects on the output particle size distribution of roll gap, roll disposition, wheat kernel hardness, moisture content and shape to be quantified (Campbell and Webb, 2001; Campbell *et al.*, 2001, 2007, 2012; Fang and Campbell, 2003a,b; Fuh *et al.*, 2014). The objectives of the current work are to demonstrate that continuous breakage functions can also be defined in relation to particle composition, for use alongside breakage functions that predict particle size distribution, and to generate experimental data to begin to identify the form and significance of those functions and the new insights they reveal. The current work thus represents the continuous equivalent of the discrete compositional breakage matrices introduced by Fistes and Tanovic (2006).

Theory

The breakage equation for roller milling of wheat in its cumulative form is

$$P_2(x) \quad = \quad \int_0^{\infty} B(x, D)\rho_1(D)dD \qquad (1)$$

where D is the input particle size, x is the output particle size, $P_2(x)$ is the proportion by mass of output material smaller than size x, $B(x, D)$ is the breakage function and $\rho_1(D)$ is the probability density function describing the input particle size distribution (Campbell *et al.*, 2007). The logic of the breakage equation is that the total mass of particles smaller than a given size x arises from contributions from all the inlet particles. The contribution from inlet particles initially of size D depends on how many of those particles there are (which is quantified by $\rho_1(D)$) and on how those particles break (which is quantified by the breakage function, $B(x, D)$). The total mass is found by integrating all of these contributions over the range of inlet particle sizes.

Applying equivalent logic, the composition of particles can also be described and related to the particle size distribution. Choomjaihan (2009) derives the relationships by proposing that the entire wheat kernel, and its milled fractions, can be considered to be made up of four main components: Pericarp (including testa and nucellar tissue), Aleurone, Starchy Endosperm and Germ. The sum of the proportions of these four components is unity:

$$X_{pe} + X_{al} + X_{en} + X_{ge} \quad = \quad 1 \qquad (2)$$

where X_{pe} is the proportion of the whole wheat that is Pericarp, X_{al} is the proportion of the whole wheat that is Aleurone, X_{en} is the proportion of the whole wheat that is Endosperm, and X_{ge} is the proportion of the whole wheat that is Germ. Typically X_{pe} would be about 8%, X_{al} about 7%, X_{en} about 82% and X_{ge} about 3% (Pomeranz, 1988).

On breakage, particles are formed that individually may contain Pericarp, Aleurone, Endosperm and Germ in different proportions. In general, the particles in a size range, say from 100-200 μm, will have a proportion of each component that will be different from particles in a different size range, say 2000-2100 μm; the smaller particles are likely to contain more Endosperm material, the larger particles more bran material (*i.e.* Pericarp and Aleurone).

Consider the total proportion of outlet particles smaller than size x, given by $P_2(x)$. These particles, as a whole, are made up of a proportion of Pericarp, a proportion of Aleurone, a proportion of Endosperm, and a proportion of Germ. The total amount of particles smaller than size x is made up of the total Pericarp that is in particles smaller than size x, plus the total Aleurone that is in particles smaller than x, plus the total Endosperm that is in particles smaller than x, plus the total Germ that is in particles smaller than x. Mathematically:

$$\begin{aligned} P_2(x) &= \frac{\text{total mass of particles smaller than } x}{\text{total mass}} \\ &= \sum_i X_i \cdot Y_i(x) \\ &= X_{pe} \cdot Y_{pe}(x) + X_{al} \cdot Y_{al}(x) + X_{en} \cdot Y_{en}(x) + X_{ge} \cdot Y_{ge}(x) \end{aligned} \tag{3}$$

where $Y_{pe}(x)$ is the proportion (by mass) of the total Pericarp that is in particles smaller than x, and so on for $Y_{al}(x)$, $Y_{en}(x)$ and $Y_{ge}(x)$. Figure 1 illustrates how the distributions of the four components sum to give the total particle size distribution. Figure 2 illustrates the distributions in their non-cumulative forms. (Note that in Figures 1 and 2, the proportions of the four components are unrealistic, having been set at 20%, 10%, 67% and 3% arbitrarily, just to separate out the lines in order to illustrate the point. The shapes of the curves are also arbitrary, contrived to show Endosperm predominantly breaking into small particles, Pericarp and Aleurone staying in larger particles, and Germ forming a narrow peak within the mid-range particles.)

For example, consider the more realistic situation that in the whole wheat, $X_{pe} = 0.08$, $X_{al} = 0.07$, $X_{en} = 0.82$, $X_{ge} = 0.03$. The wheat is milled, forming particles ranging in size from 0 up to 4000 μm, with most of the particles at the smaller end of the range. Consider just those particles that are smaller than 500 μm. Imagine that 40% of the total Pericarp has ended up in those particles; the other 60% is in particles that have remained larger than 500 μm. However, the Aleurone has not broken so readily, so only 30% of the total Aleurone has ended up in the particles smaller than 500 μm; 70% of the Aleurone has stayed in the larger particles. The Endosperm has broken easily; 80% of the Endosperm is now in small particles, with only 20% in large particles. Meanwhile, the Germ is evenly split; half of the Germ material is in particles that are smaller than 500 μm. Thus:

$$Y_{pe}(500) = 0.40,\ Y_{al}(500) = 0.30,\ Y_{en}(500) = 0.80,\ Y_{ge}(500) = 0.50$$

Then, the total proportion of particles smaller than 500 μm is given by

$$\begin{aligned} P_2(x) &= 0.08\times 0.4 + 0.07\times 0.3 + 0.82\times 0.8 + 0.03\times 0.5 \\ &= 0.032 + 0.021 + 0.656 + 0.015 \\ &= 0.724 \end{aligned}$$

i.e. 72.4% of particles are smaller than 500 μm. Taking these particles as a whole, they are made up of 0.032/0.724=4.4% Pericarp, 2.9% Aleurone, 90.6% Endosperm and 2.1% Germ, *i.e.* they are enriched in Endosperm, and depleted in the other components, compared with the material as a whole.

This is a contrived example, to illustrate the mathematics, but it reflects the known behaviour of wheat during breakage, that bran material (Pericarp and Aleurone) tends to stay in large particles, while endosperm shatters more readily into smaller particles. Thus, separation on the basis of size using repeated milling and sifting allows separation of the bran from endosperm to produce relatively pure white flour. As in the contrived example here, one would expect smaller particles to be enriched in endosperm material, compared with the endosperm content of the whole wheat.

Now, taking the Pericarp as an example, the Pericarp concentration in this group of particles, $Y^*_{pe}(x)$, is given by the total amount of Pericarp in particles smaller than x, divided by the total amount of particles smaller than x. The latter is the sum of the individual components, hence:

$$\begin{aligned} Y^*_i(x) &= \frac{\text{mass of component } i \text{ in particles smaller than } x}{\text{total mass in particles smaller than } x} \\ &= \frac{X_{pe}\cdot Y_{pe}(x)}{P_2(x)} \\ &= \frac{X_{pe}\cdot Y_{pe}(x)}{X_{pe}\cdot Y_{pe}(x) + X_{al}\cdot Y_{al}(x) + X_{en}\cdot Y_{en}(x) + X_{ge}\cdot Y_{ge}(x)} \end{aligned} \tag{4}$$

$$\begin{aligned} Pe'(x) &= \frac{Pe_{tot}\times Pe(x)}{P_2(x)} \\ &= \frac{Pe_{tot}\times Pe(x)}{Pe_{tot}\times Pe(x) + Al_{tot}\times Al(x) + En_{tot}\times En(x) + Ge_{tot}\times Ge(x)} \end{aligned} \tag{5}$$

and similarly for the concentrations of the other components, defined as $Y^*_{al}(x)$, $Y^*_{en}(x)$ *and* $Y^*_{ge}(x)$. Similarly to X_i, the sum of all Y^*_i concentrations must be unity:

$$\sum_i Y^*_i(x) = Y^*_{pe}(x) + Y^*_{al}(x) + Y^*_{en}(x) + Y^*_{ge}(x) = 1 \tag{6}$$

Referring to Figure 1, $X_{pe}(x)$ is defined by the point A divided by the point C (the amount of Pericarp in particles smaller than x divided by the total amount of Pericarp), while $Y^*_{pe}(x)$ is defined by the point A divided by the point B (the amount of Pericarp in particles smaller than x divided by the total amount of particles smaller than x, *i.e.* the average concentration of Pericarp in particles smaller than x). Note that this is the average concentration across all of the particles smaller than x. The concentration of Pericarp in particles of size x will be different from this average. We turn our attention to this now.

The preceding paragraphs have focussed on cumulative probability density functions. The probability density function for component i in its non-cumulative form, $\rho_i(x)$, is defined as:

$$\rho_i(x) \quad = \quad \frac{d}{dx} Y_i(x) \tag{7}$$

The quantity $\rho_i(x)dx$ is the proportion of the total component i that is in particles of size x, $x+dx$. Multiplying this by the total proportion of component i in the material as a whole gives the total of the material as a whole that is component i and that is in the size range x, $x+dx$. This is equal to the proportion of total material in the size range x, $x+dx$, multiplied by the component i concentration of that material. Figure 2 illustrates for Pericarp the two ways of defining this quantity of material, based on the particle size distribution and composition, or on the Pericarp total and distribution, showing that they are equivalent. This equivalence is expressed mathematically as:

$$X_i \rho_i(x)dx = \rho_2(x) y_i(x)dx \tag{8}$$

where $\rho_2(x)$ is the probability density function describing the outlet particle size distribution, and $y_i(x)$ is the concentration of component i in particles of size x. Thus the amount of material defined by the brown area in Figure 2 is the value of the probability density function for Pericarp at that point, $\rho_{pe}(x)$, multiplied by dx and by the total proportion of Pericarp, X_{pe}. This is equal to the total amount of material in the range $x+dx$ multiplied by the concentration of Pericarp in that total, $y_{pe}(x)$.

Similarly, $y_{al}(x)$ is the concentration of Aleurone material, $y_{en}(x)$ is the concentration of Endosperm material and $y_{ge}(x)$ is the concentration of Germ material in particles of size x. Clearly

$$\sum_i y_i(x) = y_{pe}(x) + y_{al}(x) + y_{en}(x) + y_{ge}(x) = 1 \tag{9}$$

and

$$\sum_i X_i \rho_i(x) = \rho_2(x) \sum_i y_i(x) = \rho_2(x) \tag{10}$$

The breakage equation is given by Eqn. (1). If D is essentially monodispersed (little variation in wheat kernel size), then the breakage is described by $P_2(x) = B(x,D)$ or, more generally, by $B(x,G/D)$ – the proportion of particles smaller than x arising from breakage of wheat at a given milling ratio G/D, where G is the roll gap. The functions $y_i(x)$ similarly become $y_i(x,G/D)$, the proportion of botanical component i in particles of size x resulting from milling wheat at a milling ratio G/D. If the $y_i(x,G/D)$ are known, then both the size distribution of particles following breakage and their compositions can be predicted. Thus the compositional breakage equation is:

$$\begin{aligned} P_2(x,G/D) &= \sum_i X_i \cdot Y_i(x,G/D) = \sum_i X_i \cdot \int_0^x \rho_i(x,G/D) \cdot dx \\ &= \sum_i \int_0^x \rho_2(x,G/D) \cdot y_i(x,G/D) \cdot dx \end{aligned} \tag{11}$$

and in its non-cumulative form:

$$\begin{aligned} \rho_2(x,G/D) &= \sum_i X_i \cdot \rho_i(x,G/D) \\ &= \sum_i \rho_2(x,G/D) \cdot y_i(x,G/D) \end{aligned} \tag{12}$$

Equations 11 and 12 allow both the particle size distribution, and the composition of each size fraction, to be described by a single equation. This simplifies the problem to establishing "concentration functions" to describe $y_{pe}(x,G/D)$, $y_{al}(x,G/D)$, $y_{en}(x,G/D)$ and $y_{ge}(x,G/D)$, leading to "compositional breakage functions" that describe $\rho_{pe}(x,G/D)$, $\rho_{al}(x,G/D)$, $\rho_{en}(x,G/D)$ and $\rho_{ge}(x,G/D)$. This could be done by milling wheat at different roll gaps, sifting it into difference size fractions, and measuring the compositions of those size fractions, *i.e.* the relative proportions of Pericarp, Aleurone, Endosperm and Germ in each fraction. Knowing how these relative compositions change, curves could then in principle be fitted to describe these changes as functions of x and G/D. Ultimately, of course, with a very large experimental programme, these compositional breakage functions could be extended to include hardness, as Campbell *et al*. (2007) did for the size-based breakage function. These ambitions were beyond the scope of the current work.

Equations 11 and 12 represent the continuous equivalent of the discrete compositional breakage matrices introduced by Fistes and Tanovic (2006). The equations presented here are continuous functions that are more generally applicable and more readily interpretable.

Identifying the form of compositional breakage functions

Having derived the compositional breakage equation above, the first objective of the current work, the second objective is to begin to understand the form of the compositional breakage functions by generating experimental data. In principle this is as simple as measuring the concentrations of Pericarp, Aleurone, Endosperm and Germ in size fractions following milling, and fitting functions to describe the variation. However, there are two difficulties with this. Firstly, these concentration functions are not probability density functions and hence do not have the well defined constraints of probability density functions that allow easy fitting. Secondly, measuring the proportions of these materials in milled wheat samples is not straightforward.

Taking the first of these issues, Eqn. (8) can be rearranged to give

$$y_i(x) \quad = \quad \frac{X_i \rho_i(x)}{\rho_2(x)} \tag{13}$$

where

$$\rho_2(x) \quad = \quad \frac{d}{dx} P_2(x) \tag{14}$$

and $\rho_i(x)$ is similarly the derivative of $Y_i(x)$ as defined in Eqn. 7. Campbell *et al.* (2012) introduced the Double Normalised Kumaraswamy Breakage Function (DNKBF) as a flexible probability density function well suited to describing the particle size distributions arising from roller milling of wheat, and having a cumulative form that is easy to fit and is then differentiable. Assuming this function has the flexibility to describe $Y_i(x)$ as well, from which $\rho_i(x)$ could be obtained by differentiation, Eqn. 13 then allows $y_i(x)$, the concentration of component i in particles of size x, to be calculated as the ratio of these two probability density functions. This approach, involving fitting a cumulative probability density function to the accumulated data, is likely to deal with inaccuracies in the experimental data more effectively, and to yield more meaningful descriptions of the compositional breakage functions, than attempting to fit the concentration data directly.

The second issue identified above is that of experimentally measuring the composition of milled fractions. In principle this can be done using suitable biochemical markers specific for each tissue type (Peyron et al., 2002; Barron *et al.*, 2007; Barron and Rouau, 2008; Hemery *et al.*, 2009; Barron *et al.*, 2011). However, Barron (2011) predicted the relative tissue proportion in wheat mill streams by FTIR spectroscopy and PLS analysis. In that study, Aleurone Layer, Intermediate Layer (composed of three layers: hyaline layer, testa and inner pericarp (Barron *et al.*, 2007; Barron, 2011), Outer Pericarp and Starchy Endosperm were isolated as in previous works from the same author from various common wheat cultivars. (Germ constitutes about 3% of the grain; its omission adds an error of a magnitude that is within the analytical error of the method.) Different milled streams arising from debranning, conventional milling and bran fractionation were produced from two French wheat varieties. The spectra of botanical tissues and milled fractions were collected with a FTIR coupled with an ATR device. The biochemical markers technique studied by the same author was used as the reference method (Barron *et al.*, 2007; Hemery *et al.*, 2009; Barron *et al.*, 2011). PLS models were developed to predict the proportion of the botanical tissues in the milled streams. The predictions obtained were good despite the complex natures and compositions of botanical tissues. These models were used in the current work to quantify the compositions of milled fractions in order to fit compositional breakage functions.

Materials and Methods

In order to demonstrate the compositional breakage equation approach, in the current work a hard UK wheat, Mallacca (average hardness = 52.5, average mass = 47.6 mg, average diameter = 3.26 mm after conditioning, as measured by the Single Kernel Characterisation System Model 4100 (Perten Instruments, Sweden)) and a UK soft wheat, Consort (SKCS hardness = 33.9, average mass = 34.7 mg, average diameter = 2.89 mm after conditioning) were conditioned to 16% moisture (wet basis). 100 g samples were milled on the Satake STR100 mill (Satake Corporation, Hiroshima, Japan) at a roll gap of 0.5 mm under Sharp-to-Sharp (S-S) and Dull-to-Dull (D-D) dispositions, and separated by sifting into eight fractions using sieves of size 2000, 1700, 1400, 1180, 850, 500 and 212 μm, using equipment and methods described elsewhere (Campbell *et al.*, 2007). The milled fractions were analysed using Barron's spectroscopy-based models, in order to estimate the proportions of Outer Pericarp, Intermediate Layer, Aleurone and Starchy Endosperm in each fraction. In total 34 samples were analyzed: two wheat types × two dispositions × one roll gap × eight fractions = 32, plus the two whole wheats = 34. This work is presented more fully in Galindez-Najera (2014). No replication was undertaken due to practical limitations; within the constraints of the work, we preferred to generate data from contrasting wheats and milling conditions, to serve the purposes of illustrating the approach and allowing tentative new insights.

The protocol for spectroscopic analysis of the samples was based on the method described by Barron (2011): milled fractions were first ground in liquid nitrogen with a Spex CertiPrep 6750 laboratory impact grinder to have a homogenous size. Spectra were recorded in the MIR region using a Nicolet Nexus 6700 (ThermoScientific, Courtaboeuf, France) spectrometer equipped with an ATR Smart DuraSampleIR accessory (ThermoScientific, U.K.) and a Mercury Cadmium-Telluride-High D detector. Spectra were recorded between 800 and 4000 cm^{-1}, with samples pressed onto the diamond ATR area. Interferograms (128) were collected at 4 cm^{-1} resolution and co-added before Fourier transformation. For each sample five spectra were collected. An air-background scan was recorded every three spectra. Partial Least Square (PLS) quantification was applied using models developed by Barron (2011). Similar spectral pre-treatments were then applied to predict each tissue proportion. Outer Pericarp, Intermediate Layer (including inner pericarp), Aleurone and Starchy Endosperm were predicted in each milled fraction, and the results interpreted through the compositional breakage equation.

A number of cautions are emphasised at this point. Firstly, we acknowledge that the correlations used in the model were based on French wheats, such that the absolute results generated for these UK samples are unlikely to be accurate. However, the relative values are likely to be sufficiently meaningful to allow the approach here to be demonstrated and to yield valid insights. Secondly, the models do not allow quantification of the Germ, and they distinguish between the Outer Pericarp and the Intermediate Layer. The information they provide is therefore not quite in the form of the derivations above, in particular not intending to provide mutually exclusive proportions of components that sum to unity. The values for Outer Pericarp, for example, should be considered to indicate how the Outer Pericarp concentration varies with particle size, but the corresponding variations of Intermediate Layer, Aleurone and Endosperm are not expected to sum to one. Thus the data can be used in conjunction with Eqn. 12 to find the form of the compositional breakage functions but not their absolute values, and could not be used at this stage to define completely Eqn. 11, the compositional breakage equation. We also acknowledge that the individual trials were not replicated.

Results and Discussion

Table 1 shows the proportion of material on each sieve size following milling under S-S or D-D, and the percentages of Outer Pericarp, Intermediate Layer, Aleurone and Starchy Endosperm in each fraction as predicted by Barron's model, along with the predictions for each component in whole wheat samples. Note that the independent raw data for each component did not sum to unity, due to inherent errors in the predictions and in their application to UK wheats; on average the total material was overestimated by 8.3% for the Mallacca samples and 4.9% for Consort, possibly suggesting that the French wheats used to generate the models were more similar to the soft Consort wheat, although the discrepancy is within the accuracy of the method. The data reported in Table 1 have been normalised to unity, as a reasonable approximation to the composition of particles in each size range, and to fit the assumptions underlying the formulation of the compositional breakage equation.

The total percentage of each component in the whole Mallacca wheat was X_{pe} = 8.3%, X_{Inlay} = 1.2%, X_{al} = 6.0% and X_{en} = 84.4%; and in the whole Consort wheat was X_{pe} = 2.3%, X_{Inlay} = 2.9%, X_{al} = 5.8% and X_{en} = 88.9%. Multiplying the amount of material on each sieve by the concentration of a given component, and summing these, allows the cumulative compositional distributions, $Y_{pe}(x)$, $Y_{al}(x)$, $Y_{en}(x)$ and $Y_{Inlay}(x)$ (the proportion by mass of the total botanical component that is in particles smaller than x) to be calculated.

The total is reported as the average for each component in Table 1, for each wheat type under each milling disposition. Ideally, these averages would be the same under both dispositions, and identical with the predicted compositions of the whole grains. Inspection of Table 1 shows that there are some significant discrepancies, which underline again the inherent errors in the prediction method and in its application to UK wheats. Nevertheless, the data allow the compositional breakage function approach to be demonstrated, with appropriate caution, and using the averages rather than the data for whole wheat in order to ensure internal consistency in the analysis. The justification for this is that the average values are averaged from eight measurements, compared with just one for the whole wheat samples, and that in any case the PLS models were developed for milled stocks rather than for whole wheats

(Barron, 2011), so the results for the milled fractions might be expected to be more accurate than those for the whole wheats.

Figure 3 shows the cumulative distributions for the particle size distribution and for the four component distributions, for the Mallacca wheat milled under a Sharp-to-Sharp disposition. Figure 4 presents the experimental data and the fitted size distributions in their non-cumulative forms. Table 2 reports the fitted Double Normalised Kumaraswamy Breakage Function parameters. In order to fit the DNKBF, the *x*-axis was normalised by dividing particle size by 4000 μm, in order to yield Kumaraswamy shape parameters consistent with previously reported work, although the current work only used 2000 μm for its largest sieve, so the data beyond this size is not available. The DNKBF in its cumulative form is (Campbell *et al.*, 2012)

$$P_2(z) = \underbrace{\alpha\left(1-\left(1-z^{m_1}\right)^{n_1}\right)}_{\text{Type 1 Breakage}} + \underbrace{\left(1-\alpha\right)\left(1-\left(1-z^{m_2}\right)^{n_2}\right)}_{\text{Type 2 Breakage}} \tag{15}$$

where z is the normalized size, $P(z)$ is the percentage smaller than z, α is the proportion of the distribution that can be described as Type 1 breakage, and m_1 and n_1 are parameters corresponding to Type 1 breakage. The quantity ($1-\alpha$) gives the proportion of Type 2 breakage, while m_2 and n_2 are the parameters that describe the form of Type 2 breakage. Differentiating Eqn. 14 gives the non-cumulative form of the DNKBF:

$$p_2(z) = \underbrace{\alpha\left(m_1 n_1 z^{m_1-1}\left(1-z^{m_1}\right)^{n_1}\right)}_{\text{Type 1 Breakage}} + \underbrace{\left(1-\alpha\right)\left(m_2 n_2 z^{m_2-1}\left(1-z^{m_2}\right)^{n_2}\right)}_{\text{Type 2 Breakage}} \tag{16}$$

Considering the particle size distributions in Figure 3(a) and Figure 4(a), the DNKBF describes the data well, yielding values of $\alpha = 0.36$, $m_1 = 5.54$, $n_1 = 178.10$, $m_2 = 1.08$ and $n_2 = 3.44$; these values are broadly consistent with previous work for a wheat of hardness around 50 milled under S-S (Campbell *et al.*, 2012).

Figures 3(a) and 4(a) also show the Type 1 and Type 2 functions that combine to give the DNKBF. The values of m_1 and n_1 describe a narrow peak of mid-range particles, while those for m_2 and n_2 describe a broad distribution of mostly small particles but extending to include the very large particles. Galindez-Najera and Campbell (2014) described a mechanism for Type 2 breakage that explains the co-production of the very large bran particles and the small Endosperm particles, and hence why they are described by the same Type 2 breakage function.

Considering now the cumulative distribution shown for the Outer Pericarp material in Figure 3(b) and the non-cumulative form in Figure 4(b), again the DNKBF describes the data well. Comparing Figures 4(a) and 4(b), it appears that the Outer Pericarp is noticeably concentrated in the mid-range particles. The DNKBF shape parameters are m_1 = 4.05, n_1 = 53.9, m_2 = 0.38 and n_2 = 0.91, with the proportion of Type 1 breakage, α = 0.733. The decrease in the Type 1 parameters has tended to make the Type 1 component of the distribution more narrow, while the proportion of Type 1, α, has increased to 0.733. Thus, Outer Pericarp is predominantly found in the mid-range Type 1 particles resulting from breakage. This is a new insight into wheat breakage.

The Type 2 parameters have both decreased to well below 1, giving a very steep peak for the very small particles, matching the experimental data at that point. This suggests that there is a significant amount of Outer Pericarp in the very small particles. This can be understood as Pericarp "dust" that is produced during breakage. Although bran material (Pericarp and Aleurone) tends to stay as large particles during roller milling, inevitably some small particles of bran (Outer Pericarp or beeswing) are produced, and this is evident here in the experimental data and in the modelling of it. Again, this is a new insight that is consistent with the accepted physical understanding of the nature of wheat breakage, but here has for the first time been identified and described quantitatively. It is proposed cautiously at this point, recognising that this work is for a single wheat and so far we have considered only a single component and only the S-S data. But it serves at this point to illustrate the nature of the compositional breakage function interpretation and the insights that can result.

Moving to consider the results for the Aleurone layer, Figures 3(d) and 4(d) show very similar results to those for Outer Pericarp; this makes sense, as the Pericarp and Aleurone tend to fuse during conditioning and break together (Hemery *et al.*, 2007). The fit is not quite as good as for the Outer Pericarp, despite the spectroscopic model being in general more accurate for Aleurone than for Outer Pericarp (Barron, 2011). Nevertheless, the same features are evident: a greater concentration of Aleurone material in mid-range Type 1 particles, and a similar spike of very small particles of Aleurone-containing "dust". The proportion of Type 1 in this case is lower at 0.557, while m_1 = 5.20, n_1 = 100, m_2 = 0.63 and n_2 = 2.13, all larger than the corresponding values for Outer Pericarp. Not too much should be read into the fine detail of these changes, beyond noting that in general the increases in the values of the Kumaraswamy shape parameters move the distribution slightly to the right. This may suggest the Aleurone is more prevalent in slightly larger particles following breakage – possibly Outer Pericarp, being on the outside, is “knocked off” these larger particles more easily than Aleurone, although a physical mechanism is not obvious and the data does not support excessive speculation at this point. However the more general point that the compositional variation of particles is very similar for both the Outer Pericarp and Aleurone, and information from these two different components points to similar conclusions regarding the nature of mid-range particles and the production of bran dust.

Figures 3(c) and 4(c) show the results for the Intermediate Layer. This data is predicted by the spectroscopic model least accurately, such that there is significant scatter in the data, but the results show a similar pattern to those for Outer Pericarp and Aleurone, adding confidence that the features apparent in the graphs for these two components are genuine.

Moving to Figures 3(e) and 4(e), the Starchy Endosperm shows contrasting behaviour to the Outer Pericarp and Aleurone, being more predominant in the smaller particles, but with the fitted curves featuring a dip at the very smallest particles, consistent with these particles containing significant amounts of bran dust and hence less endosperm. The proportion of Type 1 is 0.293, with m_1 = 6.30, n_1 = 343, m_2 = 1.18 and n_2 = 3.98. The increase of m_2 to >1 introduces the hump at the lower end of the Type 2 curve. There is still a significant Type 1 bump in the middle of the distribution, indicating that there is a lot of Endosperm material in these mid-range Type 1 particles. This is for the simple reason that there are a lot of these Type 1 particles. We must remember that these distributions combine the particle size distribution and the composition of those particles, such that the shapes of these curves is dominated by the shape of the overall particle size distribution. The fit to the data is good, but this data does not show clearly the concentrations of components in these particles. We will focus on the concentrations in a moment, once we have considered results for the Intermediate Layer.

As noted above, the concentration functions can be found by inserting the Double Kumaraswamy Functions fitted to the particle size distribution and to the compositional distributions into Eqn. 12. Once again this is illustrated in relation to Outer Pericarp:

$$y_i(x) = \frac{X_i \rho_i(x)}{\rho_2(x)} = \frac{X_i\left[\alpha\left(m_1 n_1 z^{m_1-1}\left(1-z^{m_1}\right)^{n_1}\right)+(1-\alpha)\left(m_2 n_2 z^{m_2-1}\right)\left(1-\left(1-z^{m_2}\right)^{n_2}\right)\right]_{i\,distribution}}{\left[\alpha\left(m_1 n_1 z^{m_1-1}\left(1-z^{m_1}\right)^{n_1}\right)+(1-\alpha)\left(m_2 n_2 z^{m_2-1}\right)\left(1-\left(1-z^{m_2}\right)^{n_2}\right)\right]_{particle\,size\,distribution}} \quad (17)$$

Figure 5 shows the concentration functions resulting from dividing the fitted DNKBF functions using Eqn. 17, for all four components, compared with the original experimental data for each component's concentration. The agreement is good, as one would hope as it is a circular relationship – the experimental data was used to generate the compositional breakage functions, so the reverse analysis (which is what the ratio of the composition and particle size DNKBFs is) would be expected more or less to recreate the experimental data. Figure 5 simply reassures that the analysis does indeed reveal genuine features, while allowing continuous functions to be formulated that could not readily be formulated from the raw compositional data.

A number of further observations can be drawn. Firstly, although dividing one wiggly function by another wiggly function gives an even more wiggly function for which not every wiggle is meaningful, the curves obtained do seem to agree with the trends in the experimental data. The curves and data beyond 2000 µm (z = 0.5) should be largely ignored, as there was only one data point covering this entire range. But below 2000 µm (z = 0.5), the concentration of Outer Pericarp as shown by the curve is high initially and drops suddenly, indicating fine Outer Pericarp dust present as very small particles; the experimental data also shows this. The concentration then increases to a peak for the mid-range particles and begins to decrease again, features that are again reflected in the experimental data.

The curves and experimental data for Aleurone show the same general pattern, albeit with more scatter. The curves and data for the Starchy Endosperm show an inverse trend with lower concentrations in the finest and the mid-range particles. The trend is less pronounced because the Endosperm necessarily dominates the composition of all the particles. Meanwhile the overall trend is downwards, consistent with the expectation that larger particles are less concentrated in Endosperm than smaller particles. The Intermediate Layer seems to show a slightly increasing trend of concentration with particle size.

A further observation is that the concentration functions are clearly very complex; it would be not be possible to define a simple function likely to be capable of describing variations in component concentration for a range of wheats milled under a range of conditions. The approach presented here, allowing the particle size distribution and the component distributions to be described by Double Kumaraswamy Functions, the ratios of which give the concentration functions, is a practical way to describe, quantify and interpret the effects of breakage on component distributions.

Figures 6 and 7 show the equivalent results for the samples milled under a Dull-to-Dull disposition. The fitted DNKBF parameters are again reported in Table 2. Although this is the same wheat, in other respects these results are independent of those discussed above; the size fractions were generated and analysed independently of those produced from milling under S-S. It is encouraging that many of the features seen in the S-S data also appear here: the higher concentrations of Outer Pericarp and Aleurone in mid-range Type 1 particles, and higher concentration of Endosperm in smaller particles. A notable difference is the absence of evidence of Outer Pericarp in the very fine dust, although there is still evidence of Aleurone material in this fine dust, and also of Intermediate Layer, while there is a high concentration of Outer Pericarp in the slightly larger small particles. This probably reflects limitations in this small set of experimental data, but could conceivably reflect differences in the nature of breakage under Dull-to-Dull compared with Sharp-to-Sharp milling. Galindez-Najera and Campbell (2014) describe differences in the scraping of bran particles formed from Dull-to-Dull milling compared with Sharp-to-Sharp. Based on this description, it is plausible that D-D gives less creation of bran dust in the first place, but yields more effective scraping of Endosperm from the inside of the large bran particles, this scraping generating Aleurone and Intermediate Layer material in the finest particles, but not getting as far as Outer Pericarp. More extensive work would be needed to identify conclusively patterns of breakage under different conditions, but the results from D-D milling support those from S-S in demonstrating the quantitative interpretation that the compositional breakage function approach can deliver.

Figure 8 presents the experimental data and the fitted size distributions in their non-cumulative forms for Consort wheat. The fitted DNKBF parameters are again reported in Table 2.

Considering the particle size distribution in Figure 8(a), the DNKBF describes the data well, yielding values of $\alpha = 0.143$, $m_1 = 8.21$, $n_1 = 1527$, $m_2 = 0.99$ and $n_2 = 2.24$; these values are broadly consistent with previous work for a wheat of hardness around 30, milled under S-S (Campbell *et al.*, 2012).

Figure 8(a) also show the Type 1 and Type 2 functions that combine to give the DNKBF. As a reminder, the values of m_1 and n_1 describe a narrow peak of mid-range particles, while those for m_2 and n_2 describe a broad distribution of mostly small particles but extending to include the very large particles.

Considering now the cumulative distribution shown for the Outer Pericarp in Figure 8(b), again the DNKBF describes the data well. Comparing Figures 8(a) and 8(b), it appears that the Outer Pericarp material is clearly concentrated in the mid-range particles. The DNKBF shape parameters are m_1 = 4.02, n_1 = 53.9, m_2 = 0.75 and n_2 = 0.63, with the proportion of Type 1 breakage, α = 0.790. The decrease in the Type 1 parameters, in general, makes the Type 1 component of the distribution narrower, while the proportion of Type 1 has increased. Thus, Outer Pericarp is predominantly found in the mid-range Type 1 particles resulting from breakage. These results are similar to the findings for Mallacca wheat.

Similar to Mallacca wheat, the Type 2 parameters for Consort wheat have both decreased to below 1, but unlike Mallacca, a very small steep spike for the very small particles is observed for Consort, matching the experimental data at that point. This suggests a little amount of Outer Pericarp "dust" in the very small particles that is produced during breakage. Although bran material tends to stay as large particles during roller milling, inevitably some small particles of bran are produced. Although this new insight is not as evident as it is for Mallacca, there is still evident in both the experimental data and in the modelling for Consort. It is proposed cautiously at this point, recognising that this work is only for two wheat types and so far only a single Consort component and only the S-S data have been considered. But it serves at this point to illustrate the nature of the compositional breakage function interpretation and the insights that can result.

Regarding the results for the Aleurone layer, Figure 8(d) show a similar pattern to those for Outer Pericarp, although unlike Outer Pericarp for Mallacca wheat, there is not a steep peak for the very small particles (less dust production). The fit is once again not quite as good as for the Outer Pericarp, despite the spectroscopic model being in general more accurate for Aleurone than for Outer Pericarp (Barron, 2011). This may indicate that Aleurone breakage during milling is less well defined than Outer Pericarp breakage. Similar to Outer Pericarp, a greater concentration of Aleurone material in mid-range Type 1 particles is evident, along with very small particles of Aleurone-containing "dust", although not showing a spike. The proportion of Type 1 in this case is lower at 0.36, while m_1 = 5.65, n_1 = 100, m_2 = 1.24 and n_2 = 2.25, all larger than the corresponding values for Outer Pericarp. In general the increase in the values of the Kumaraswamy shape parameters moves the distribution slightly to the right. This may suggest once again the Aleurone is more prevalent in slightly larger particles following breakage; possibly Outer Pericarp, being on the outside, is eliminated from these larger particles more easily than Aleurone, or, perhaps the production of Aleurone is coming from inside, in other words, the Starchy Endosperm has been scraped off, allowing the action of the rolls to reach the Aleurone.

Figure 8(c) show the results for the Intermediate Layer. As noted earlier, this data is predicted by the spectroscopic model least accurately, such that there is significant scatter in the data. However, the Intermediate Layer shows an opposite behaviour with respect to Outer Pericarp and Aleurone; the presence of Intermediate Layer material is considerable higher in the dust but lower in the mid-range particles are pushed towards the larger mid-range particles. This insight is interesting because, while the Intermediate Layer might be expected to behave similarly to Aleurone and Outer Pericarp as part of the bran layers, the data suggest that the shearing effect applied to this soft wheat causes the Intermediate Layer to crumble quite easily into small particles, while the Outer Pericarp and Aleurone on either side remain relatively intact. If true, this is a remarkable new insight into the nature of soft wheat breakage.

Figure 8(e) show for the Starchy Endosperm contrasting behaviour to the Outer Pericarp and Aleurone, being more predominant in the smaller particles. The proportion of Type 1 is 0.124, with $m_1 = 6.74$, $n_1 = 343$, $m_2 = 0.951$ and $n_2 = 2.29$. Similar to Mallacca wheat, there is a significant Type 1 bump in the middle of the distribution, indicating that there is a lot of endosperm material in these mid-range Type 1 particles. Again, this is for the simple reason that there are a lot of these Type 1 particles.

Figure 9 shows the concentration functions resulting from dividing the fitted DNKB functions using Equation 17, for all four components, compared with the original experimental data for each component's concentration. Similar to Mallacca data, the experimental Consort data was used to generate the compositional breakage functions, so the reverse analysis more or less recreates the experimental data. Similar to Mallacca wheat results, Figure 9 reassures that the analysis does indeed reveal genuine features, while allowing continuous functions to be formulated that could not readily be formulated from the raw compositional data.

Figures 10 and 11 show the equivalent results for the Consort samples milled under a D-D disposition. The fitted DNKBF parameters are again reported in Table 2.

It is well established that milling a soft wheat under a D-D disposition gives a much broader particle size distribution than milling a hard wheat under S-S (Campbell et al., 2007, 2012), and the results in Figure 10 reflect this. In terms of the compositional data, once again these data are independent from those considered above, and it is again encouraging that many of the features seen in the S-S data also appear here: the higher concentrations of Outer Pericarp and Aleurone in mid-range Type 1 particles, and higher concentration of Endosperm in smaller particles. A notable difference is the absence of Outer Pericarp in the very fine dust, although there is still evidence of Aleurone material in this fine dust. The Intermediate Layer shows a high concentration of dust in the very small particles, while in the slightly larger small particles there is higher concentration of the Intermediate Layer which then decreases in the mid-range and larger particles. It is observed that Aleurone and Intermediate layer are generating more dust than Outer Pericarp, which seems to show very little or no dust production under D-D milling. Under S-S milling, the production of Aleurone dust is less compared with D-D milling, although Outer Pericarp dust is higher and Intermediate Layer seems to be even more. All these features are in contrast to the harder Mallacca wheat, in which overall, the bran dust production is considerable higher under both dispositions compared with the soft Consort wheat, and particularly higher under D-D disposition. Consistent with the description presented by Galindez-Najera and Campbell (2014), the breakage mechanism observed here seems to suggest a more effective scraping of endosperm from the inside of the large bran particles, this scraping generating Aleurone and Intermediate Layer material in the finest particles, but not getting as far as Outer Pericarp.

Figure 12 collects the Outer Pericarp, Intermediate Layer and Aleurone distributions together on the same graph, for both wheats under both dispositions. Gathering together the data from all four conditions highlights certain consistent patterns and some distinctive differences that together give a degree of confidence that the apparent effects are genuine. Most striking is the contrast between the hard Mallacca wheat and the soft Consort wheat, which is more striking than the difference between the S-S and D-D dispositions. There are some intriguing and tantalising patterns within the compositional data for Mallacca, most notably the aleurone peak being shifted to the right compared with the Outer Pericarp peak (which is also evident for Consort under S-S), and the apparent production of Outer Pericarp/Intermediate Layer/Aleurone "dust" under S-S, but only Intermediate Layer/Aleurone dust, without Outer Pericarp, under D-D, which may point to subtleties in the mechanisms of breakage. But more striking than these small differences is the relative uniformity of the Mallacca compositions in relation to Outer Pericarp, Intermediate Layer and Aleurone, which vary in broadly consistent ways with particle size. This is in marked contrast to Consort, in which the relative proportions of these three components appear to vary substantially in particles of different size, pointing to very different breakage origins. It appears that in the hard wheat, essentially the bran layers break "together", with subsequent minor variations in composition as bits are knocked off. This is consistent with the general understanding that in hard wheats, the bran "breaks together with the endosperm" (Fang and Campbell, 2002a,b, 2003a), with the breakage patterns being dominated by the endosperm physical properties. By contrast, in the soft wheat, which naturally produces much larger bran particles (Campbell *et al.*, 2007; Greffeuille *et al.*, 2007) these large flat particles are then scraped by the rollers in ways that alter their composition profoundly, and more so under D-D than under S-S. The behaviour of these large bran particles is therefore dictated much more by the properties and structure of the bran layers than by the hardness of the endosperm.

Perhaps most interesting is the evidence that when a large flat bran particle produced from a soft wheat is scraped by the differential action of the rollers, the Intermediate Layer appears to crumble into smallish particles, while the Outer Pericarp, and to a lesser extent the Aleurone, manage to stay predominantly in large particles. This is evident under S-S, while under D-D, the contrast between the Outer Pericarp and Intermediate Layer is even more evident, with Aleurone tending more towards smaller particles in this case. This idea that the Intermediate Layer, which is physically located between the Outer Pericarp and Aleurone layers, appears to crumble into small particles whilst the layers either side remain more intact, has profound consequences for understanding the nature of wheat breakage and differences between the milling performances of different wheats. It may be that this crumbly Intermediate Layer is specific to this particular Consort sample, and not a general feature of soft wheats, in which case the implications are even more profound, particularly for Second Break milling which is devoted to scraping of large flat bran particles (Mateos-Salvador *et al.*, 2013). Variations in the breakage patterns of the Intermediate Layer could be exploited for developing wheats, or conditioning regimes, or First Break/Second Break roll gap combinations that lead to noticeably enhanced separation during Second Break milling.

Greffeuille et al. (2007) investigated the mechanical properties of the outer layers, Outer Pericarp, Aleurone and Intermediate layer, together and separately, for wheats of different hardness from near-isogenic lines. They confirmed that when these outer layers were intact as unseparated bran, they were more extensible in the soft wheats, consistent with the larger bran particles obtained from milling soft wheats. For the individual layers, they found that isolated Outer Pericarp was the least extensible layer, in agreement with earlier work by Antoine et al. (2003), and that Outer Pericarp from hard wheat was more extensible and less rigid than from soft wheat. For hard wheats, the Aleurone was the most extensible of the component tissues, while in soft wheats, the Intermediate Layer was the most extensible tissue. However, when Aleurone and Intermediate Layer were tested together as adherent tissues, layers from hard and soft wheats had almost identical mechanical properties despite the different properties of the component tissues. Crucially, they concluded that for hard wheats, "the force exerted on aleurone and intermediate layers when the Outer Pericarp breaks may lead to rupture of the other tissues and consequently of the combined outer layers" while "For soft wheat, it appears that Outer Pericarp rupture does not lead to rupture of the other two tissues". This is consistent with the current work that found that Outer Pericarp, Aleurone and Intermediate Layer tended to break together in the hard wheat but very differently in the soft wheat. Greffeuille et al. (2007) highlighted differences in adhesion between layers, as well as the inherent mechanical properties of each layer, as influencing the transmission of stresses between layers and their relative rupture patterns.

In general these results and related work (Peyron *et al.*, 2002; Antoine *et al.*, 2003; Greffeuille *et al.*, 2006) show that the mechanical properties of bran layers in hard and soft wheats vary in ways that support and help to explain the conclusion here: that bran layers tend to break together into particles of relatively uniform composition in hard wheats, while in soft wheats the bran breaks into particles that vary in their proportions of the component layers, because the component layers rupture more independently. Peyron *et al.* (2002) identify understanding of adhesion forces, structural irregularities and mechanical properties of wheat outer layers as a priority area for research into understanding wheat milling behaviour and informing wheat variety selection. The current work complements these previous studies and serves this latter goal by giving a process engineering basis for quantifying the breakage patterns of wheat tissues during milling.

Throughout this discussion we have been careful to highlight limitations in the scope and accuracy of the study, and clearly these tentative suggestions would be more conclusive if based on a wider range of wheats and roll gaps (if the scraping of large flat bran particles has such profound effects on bran particle composition, it would have been interesting to complement these results with those from a smaller roll gap, for which scraping would be expected to be more severe). Nevertheless, the observed patterns are sufficiently similar in certain respects and sufficient different in others, in ways that are consistent with the known effects of wheat hardness and disposition on breakage (Fang and Campbell, 2002a,b, 2003a; Campbell *et al.*, 2007) and with the understanding of the mechanical properties of bran layers

(Greffeuille et al., 2007), that there can be confidence that the new insights are at least plausible. A greater understanding of the subtle effects of the physical properties of bran and endosperm and their interaction with roll gap and disposition has the potential to lead to more effective wheat breeding and flour milling, including the current interest in bran fractionation to develop products enriched in certain components (Hemery et al., 2007). Meanwhile, this work has demonstrated the new insights and quantitative understanding that can be accessed through the compositional breakage equation approach.

Figure 13 shows the distributions of all four tissues (Outer Pericarp, Intermediate Layer, Aleurone and Starchy Endosperm) plotted together on the same graph, for both wheats under both dispositions. In this graph the distributions have been multiplied by the proportions of each component, such that Figure 13 is the equivalent of Figure 1. The distributions therefore add up to give the overall particle size distribution, $\rho_2(x)$, *i.e.* the figure is the graphical representation of Equation 12, the compositional breakage equation in its non-cumulative form.

Figure 13(a) and (c) shows dashed lines for the Mallacca and Consort wheats milled under S-S disposition, as examples of particles of different composition. To illustrate how compositions can be calculated, for the Mallacca wheat milled under S-S disposition, the values of the Outer Pericarp, Intermediate Layer, Aleurone and Starchy Endosperm for particles of size 500 µm (shown by the dashed line in Figure 13(a)) are:

$$X_{pe}\rho_{pe}(500) = 0.0034 \qquad X_{in}\rho_{in}(500) = 0.0010$$

$$X_{al}\rho_{al}(500) = 0.0032 \qquad X_{en}\rho_{en}(500) = 0.0707$$

$$\rho_2(500) = 0.0034 + 0.0010 + 0.0032 + 0.0707 = 0.0783$$

From these values, the composition of particles of 500 µm can be calculated:

$$\begin{aligned} y_{pe}(500) &= 0.0034/0.0783 = 0.0434 \\ y_{in}(500) &= 0.0010/0.0783 = 0.0128 \\ y_{al}(500) &= 0.0032/0.0783 = 0.0409 \\ y_{en}(500) &= 0.0707/0.0783 = 0.9029 \end{aligned}$$

i.e. these particles are 4.3% Outer Pericarp, 1.3% Intermediate Layer, 4.1% Aleurone and 90.3% Starchy Endosperm.

Similarly, using a contrasting example, for the Consort wheat milled under S-S disposition, the values of the Outer Pericarp, Intermediate Layer, Aleurone and Starchy endosperm for particles of size 1500 µm (shown by the dashed line in Figure 13(c)) are:

$$X_{pe}\rho_{pe}(1500) = 0.0078 \qquad X_{in}\rho_{in}(1500) = 0.0012$$

$$X_{al}\rho_{al}(1500) = 0.0099 \qquad X_{en}\rho_{en}(1500) = 0.0721$$

$$\rho_2(1500) = 0.0078 + 0.0012 + 0.0099 + 0.0721 = 0.0910$$

hence

$$\begin{aligned} y_{pe}(1500) &= 0.0078/0.0910 &&= 0.0857 \\ y_{in}(1500) &= 0.0012/0.0910 &&= 0.0132 \\ y_{al}(1500) &= 0.0099/0.0910 &&= 0.1088 \\ y_{en}(1500) &= 0.0721/0.0910 &&= 0.7923 \end{aligned}$$

leading to a composition for these particles of 8.6% Outer Pericarp, 1.3% Intermediate Layer, 11% Aleurone and 79.2% Starchy Endosperm, i.e. these particles are much richer in bran material and depleted in endosperm, compared with the previous example.

The approach presented here, allowing the particle size distribution and the component distributions to be described by Double Kumaraswamy Functions, the ratios of which give the concentration functions, is a practical way to describe, quantify and interpret the effects of breakage on component distributions. This approach also represents the continuous equivalent of the discrete compositional breakage matrices introduced by Fistes and Tanovic (2006), yielding greater predictive power and greater mechanistic insights in wheat breakage. More work is needed to evaluate the accuracy of the spectroscopic predictions for this sort of application, and to apply the approach to a wider range of milled samples in order to lead to more confident conceptions of the physical breakage mechanisms operating during roller milling of wheat and the compositional and structural factors influencing these.

Conclusions

The distributions of wheat kernel components within eight size fractions of Mallacca and Consort wheats milled under S-S and D-D dispositions have been quantified by PLS models developed by Barron (2011), and the concentration functions found by fitting Double

Normalised Kumaraswamy Breakage Functions to the particle size distribution and to the compositional distributions. The DNKBF was found to describe the data well for the four botanical components studied: Outer Pericarp, Intermediate Layer, Aleurone and Starchy Endosperm, for both wheat types and both dispositions. For the hard Mallacca wheat, the Outer Pericarp and Aleurone layer compositions mostly varied with particle size in similar ways, consistent with these layers fusing together as “bran” and breaking together, although with possibly a subtle difference around the production of very fine particles under D-D milling. Although the data calculated for the Intermediate Layer by the spectroscopic model was less accurate compared with the other botanical tissues, the results show a broadly similar pattern to those for Outer Pericarp and Aleurone in the Mallacca wheat, adding confidence that the features observed are genuine. However, for Consort wheat, the Intermediate Layer behaved differently from Outer Pericarp and Aleurone, suggesting a different breakage mechanism which could be associated with how wheat hardness affects breakage of the bran and the production of large flat bran particles. This finding gives new insights into the nature of wheat breakage, and the contribution of the Intermediate Layer tissues to breakage, that could have implications for wheat breeding and flour mill operation as well as bran fractionation processes to recover nutritionally enhanced fractions.

The data from both wheats under the two milling dispositions highlighted consistent patterns and some distinctive differences that together give a degree of confidence that the apparent effects are genuine. The contrast between the hard Mallacca wheat and the soft Consort wheat is more evident than the difference between the S-S and D-D dispositions. Some interesting patterns within the compositional data for Mallacca are observed, like the Aleurone peak being shifted to the right compared with the Outer Pericarp peak, which is also evident for Consort under S-S, and the apparent production of Outer Pericarp/Intermediate Layer/Aleurone dust under S-S, but only Intermediate Layer/Aleurone dust, without Outer Pericarp, under D-D, which may point to subtleties in the mechanisms of breakage. The relative uniformity of the Mallacca compositions in relation to Outer Pericarp, Intermediate Layer and Aleurone, which vary in roughly consistent ways with particle size, is notable. This is in contrast to Consort, in which the relative proportions of these three components appear to vary substantially in particles of different size, pointing to very different breakage origins.

It is suggested tentatively that in the hard wheat the bran layers break “together”, with subsequent minor variations in composition as bits are knocked off. By contrast, in the soft wheat, which naturally produces much larger bran particles, these large flat particles are then scraped in such a way that their composition changes profoundly, and more so under D-D than under S-S. The behaviour of these large bran particles is therefore dictated more by the properties and structure of the bran layers than by the hardness of the endosperm. The current work complements previous studies of the mechanical properties of bran layers by giving a quantitative process engineering basis for understanding wheat breakage mechanisms in order to inform milling practice and wheat breeding.

Acknowledgements

SPGN gratefully acknowledges the National Council of Science and Technology of Mexico (CONACyT), the Mexican Government and the Ministry of Public Education (SEP) for financial support to undertake this work. The Satake Corporation of Japan is gratefully acknowledged for its support in establishing the activities of the Satake Centre for Grain Process Engineering.

References

Antoine, C., Peyron, S., Mabille, F., Lapierre, C., Bouchet, B., Abecassis, J. and Rouau X. 2003. Individual contribution of grain outer layers and their cell wall structure to the mechanical properties of wheat bran. *J Agric Food Chem* 51:2026–2033.

Barron, C. 2011. Prediction of relative tissue proportions in wheat mill streams by Fourier Transform Mid-infrared spectroscopy. *J Agric Food Chem*. 59: 10442–10447.

Barron, C. and Rouau, X. 2008. FTIR and Raman signatures of wheat grain peripheral tissues. *Cereal Chem.* 85:619-625.

Barron, C., Surget, A. and Rouau, X. 2007. Relative amounts of tissues in mature wheat (*Triticum aestivum* L.) grain and their carbohydrate and phenolic acid composition. *J Cereal Sci*, 45:88-96.

Barron, C., Samson, M.-F., Lullien-Pellerin, V. and Rouau, X. 2011. Wheat grain tissue proportions in milling fractions using biochemical marker measurements: Application to different wheat cultivars. *J Cereal Sci*. 53:306-311.

Broadbent, S. R. and Callcott, T. G. 1956a. Coal breakage processes. I. A new analysis of coal breakage processes. *J Inst Fuel* 29:524-528.

Broadbent, S. R. and Callcott, T. G. 1956b. Coal breakage processes. II. A matrix representation of breakage. *J Inst Fuel* 29:528-539.

Broadbent, S. R. and Callcott, T. G. 1957. Coal breakage processes. IV. An exploratory analysis of the cone mill in open circuit grinding. *J Inst Fuel* 30:18-21.

Campbell, G. M. and Webb, C. 2001. On predicting roller milling performance I: The breakage equation. *Powder Technol.* 115:234-242.

Campbell, G. M., Bunn, P. J., Webb, C. and Hooks, S. C. W. 2001. On predicting roller milling performance II: The breakage function. *Powder Technol*. 115:243:255.

Campbell, G. M., Fang, C. and Muhamad, I. I. 2007. On predicting roller milling performance VI: Effect of kernel hardness and shape on the particle size distribution from first break milling of wheat. *Food Bioprod Process.* 85:7-23.

Campbell, G. M., Sharp, C., Wall, K., Mateos-Salvador, F., Gubatz, S., Huttly, A. and Shewry, P. 2012. Modelling wheat breakage during roller milling using the Double Normalised Kumaraswamy Breakage function: Effects on kernel shape and hardness. *J Cereal Sci.* 55:415-425.

Choomjaihan, P. 2009. Extending the breakage equation on first break milling of wheat to include particle composition. PhD thesis. The University of Manchester, UK.

Fang, C. and Campbell, G. M. 2002a. Effect of roll fluting disposition and roll gap on breakage of wheat kernels during first break roller milling. *Cereal Chem* 79:518-522.

Fang, C. and Campbell, G. M. 2002b. Stress-strain analysis and visual observation of wheat kernel breakage during roller milling using fluted rolls. *Cereal Chem* 79:511-517.

Fang, C. and Campbell, G. M. 2003a. On predicting roller milling performance IV: Effect of roll disposition on the particle size distribution from first break milling of wheat. *J Cereal Sci* 37:21-29.

Fang, C. and Campbell, G. M. 2003b. On predicting roller milling performance V: Effect of moisture content on the particle size distribution from first break milling of wheat. *J Cereal Sci* 37: 31-41.

Fistes, A. and Tanovic, G. 2006. Predicting the size and compositional distributions of wheat flour stocks following first break roller milling using the breakage matrix approach. *J Food Eng* 75:527-534.

Fuh, K. F., Coate, J. M. and Campbell, G. M. 2014. Effects of roll gap, kernel shape and moisture on wheat breakage modelled using the Double Normalised Kumaraswamy Breakage Function. *Cereal Chem* 91:8-17.

Galindez-Najera, S. P. and Campbell, G. M. 2014. Modelling first break milling of debranned wheat using the Double Normalised Kumaraswamy Breakage function. *Cereal Chem* 91, 533-541.

Galindez-Najera, S. P. 2014. A compositional breakage equation for first break roller milling of wheat. PhD thesis. The University of Manchester, UK.

Greffeuille, V., Abecassis, J., Lapierre C. and Lullien-Pellerin, V. 2006. Bran Size Distribution at Milling and Mechanical and Biochemical Characterization of Common Wheat Grain Outer Layers: A Relationship Assessment. *Cereal Chem* 83:641-646.

Greffeuille, V., Mabille, F., Rousset, M., Oury, F.-X., Abecassis, J., Lullien-Pellerin, V. 2007. Mechanical properties of outer layers from near-isogenic lines of common wheat differing in hardness. *J Cereal Sci* 45, 227–235.

Hemery, Y., Rouau, X., Lullien-Pellerin, V., Barron, C. and Abecassis, J. 2007. Dry processes to develop wheat fractions and products with enhanced nutritional quality. *J Cereal Sci* 46:327-347.

Hemery, Y., Lullien-Pellerin, V., Rouau, X., Abecassis, J., Samson M-F., Aman, P., von Reding, W., Spoerndli, C. and Barron, C. 2009. Biochemical markers: Efficient tools for the assessment of wheat grain tissue proportions in milling fractions *J Cereal Sci* 49:55-64.

Mateos-Salvador, F., Sadhukhan, J. and Campbell, G. M., 2013. Extending the Normalised Kumaraswamy Breakage function of roller milling of wheat flour stocks to Second break. *Powder Technol* 237:107-116.

Peyron, S., Surget, A., Mabille, F., Autran, J.C., Rouau, X. and Abecassis, J. 2002. Evaluation of tissue dissociation of durum wheat grain (*Triticum durum* Desf.) generated by the milling process. *J Cereal Sci* 36:199-208.

Pomeranz, Y. 1988. Wheat Chemistry and Technology II, 3rd Edition. American Association of Cereal Chemists. St Paul, MN, USA, pp285-328.

Table 1. Particle size distributions and compositions of size fractions following milling of Mallacca and Consort wheats under Sharp-to-Sharp and Dull-to-Dull dispositions.

Sieve Size (μm)	Percentage on sieve	Pericarp concentration (%)	Intermediate Layer concentration (%)	Aleurone concentration (%)	Starchy Endosperm concentration (%)
Mallacca					
Sharp-to-Sharp					
2000	7.92	12.6	5.5	6.6	75.4
1700	10.78	11.4	2.0	11.4	75.3
1400	19.49	11.7	1.6	6.1	80.6
1180	12.87	13.9	2.4	8.9	74.8
850	14.88	12.7	1.1	5.5	80.7
500	14.09	6.5	2.0	2.4	89.2
212	10.88	3.9	0.7	7.0	88.4
0	9.10	9.2	1.9	9.7	79.2
Average		10.4	2.0	6.9	80.8
Dull-to-Dull					
2000	35.74	8.9	3.6	5.2	82.3
1700	11.66	15.2	3.0	7.1	74.7
1400	10.35	14.2	0.9	8.5	76.4
1180	5.14	13.3	2.7	3.6	80.4
850	6.47	8.9	2.5	2.1	86.4
500	10.75	5.7	1.7	5.1	87.5
212	11.06	7.8	0.0	4.5	87.7
0	8.83	2.1	4.1	7.3	86.5
Average		9.3	2.6	5.6	82.5
Whole grain		8.3	1.2	6.0	84.4
Consort					
Sharp-to-Sharp					
2000	17.93	3.8	3.5	11.0	81.8
1700	10.35	5.6	2.3	13.0	79.1
1400	14.37	7.2	2.8	11.7	78.3
1180	10.39	9.8	0.0	8.2	82.0
850	9.94	7.3	1.7	7.4	83.6
500	15.0	3.6	3.0	6.5	86.9
212	11.79	0.1	3.1	4.0	92.8
0	10.23	0.9	3.8	2.8	92.5
Average		4.7	2.6	8.3	84.4
Dull-to-Dull					
2000	37.95	6.5	3.8	15.1	74.6
1700	8.86	8.3	1.4	11.8	78.5
1400	6.91	7.0	1.4	13.2	78.4
1180	4.78	9.5	1.1	12.9	76.5
850	6.31	4.7	1.9	9.1	84.3
500	12.09	0.9	4.1	5.6	89.4
212	12.16	0.0	4.5	7.0	88.6
0	10.95	0.0	3.6	10.3	86.1
Average		4.5	3.2	11.5	80.7
Whole grain		2.3	2.9	5.8	88.9

Table 2. Fitted DNKBF parameters.

	α	m_1	n_1	m_2	n_2
MALLACCA					
Sharp-to-Sharp (S-S)					
PSD	0.358	5.54	178	1.08	3.44
Pericarp	0.733	4.05	53.9	0.38	0.91
Intermediate layer	0.374	4.81	100	0.79	1.26
Aleurone	0.558	5.18	100	0.63	2.13
Starchy endosperm	0.293	6.29	343	1.18	3.98
Dull-to-Dull (D-D)					
PSD	0.379	7.89	99.9	0.92	2.36
Pericarp	0.419	6.44	99.9	1.06	1.59
Intermediate layer	0.263	7.04	99.9	0.41	0.47
Aleurone	0.455	7.00	99.9	0.61	1.44
Starchy endosperm	0.395	8.16	99.9	0.97	2.91
CONSORT					
Sharp-to-Sharp (S-S)					
PSD	0.143	8.21	1526	0.99	2.24
Pericarp	0.790	4.02	53.9	0.75	0.63
Intermediate layer	0.421	7.24	100	1.15	7.94
Aleurone	0.356	5.65	100	1.24	2.25
Starchy endosperm	0.124	6.74	343	0.95	2.29
Dull-to-Dull (D-D)					
PSD	0.432	8.67	99.9	0.98	3.79
Pericarp	0.228	4.36	99.7	6.13	24.25
Intermediate layer	0.286	2.28	100	0.35	0.31
Aleurone	0.133	6.16	99.9	0.49	0.51
Starchy endosperm	0.421	8.56	99.9	1.03	4.93

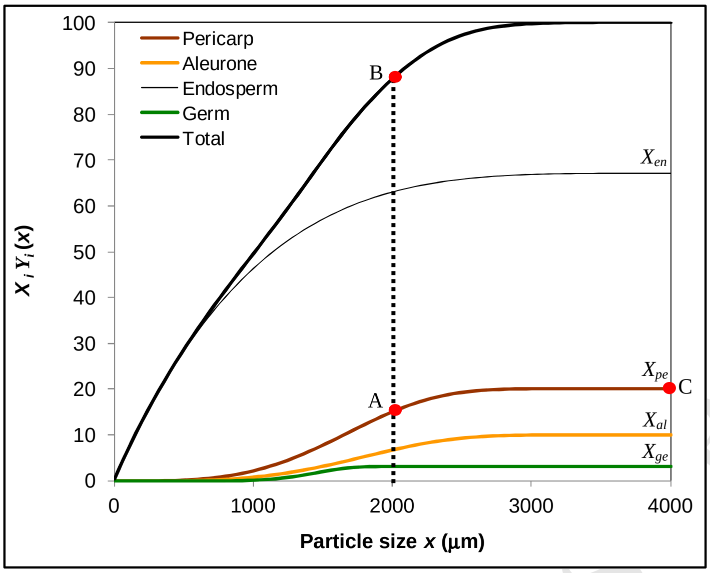

Figure 1. Contrived example that shows how the cumulative PSD is comprised of the cumulative distributions of the four botanical components in particles of different sizes. Adapted from Choomjaihan (2009).

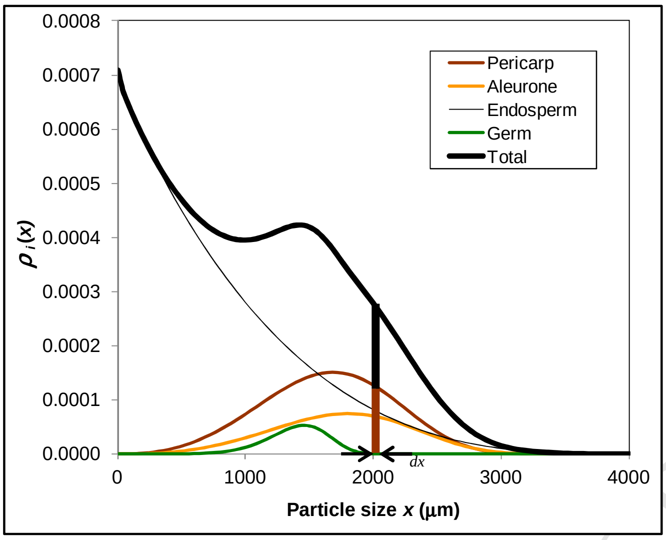

Figure 2. Non-cumulative form of the contrived example of Figure 6.1, displaying how particles of different size are made up of different compositions. Adapted from Choomjaihan (2009).

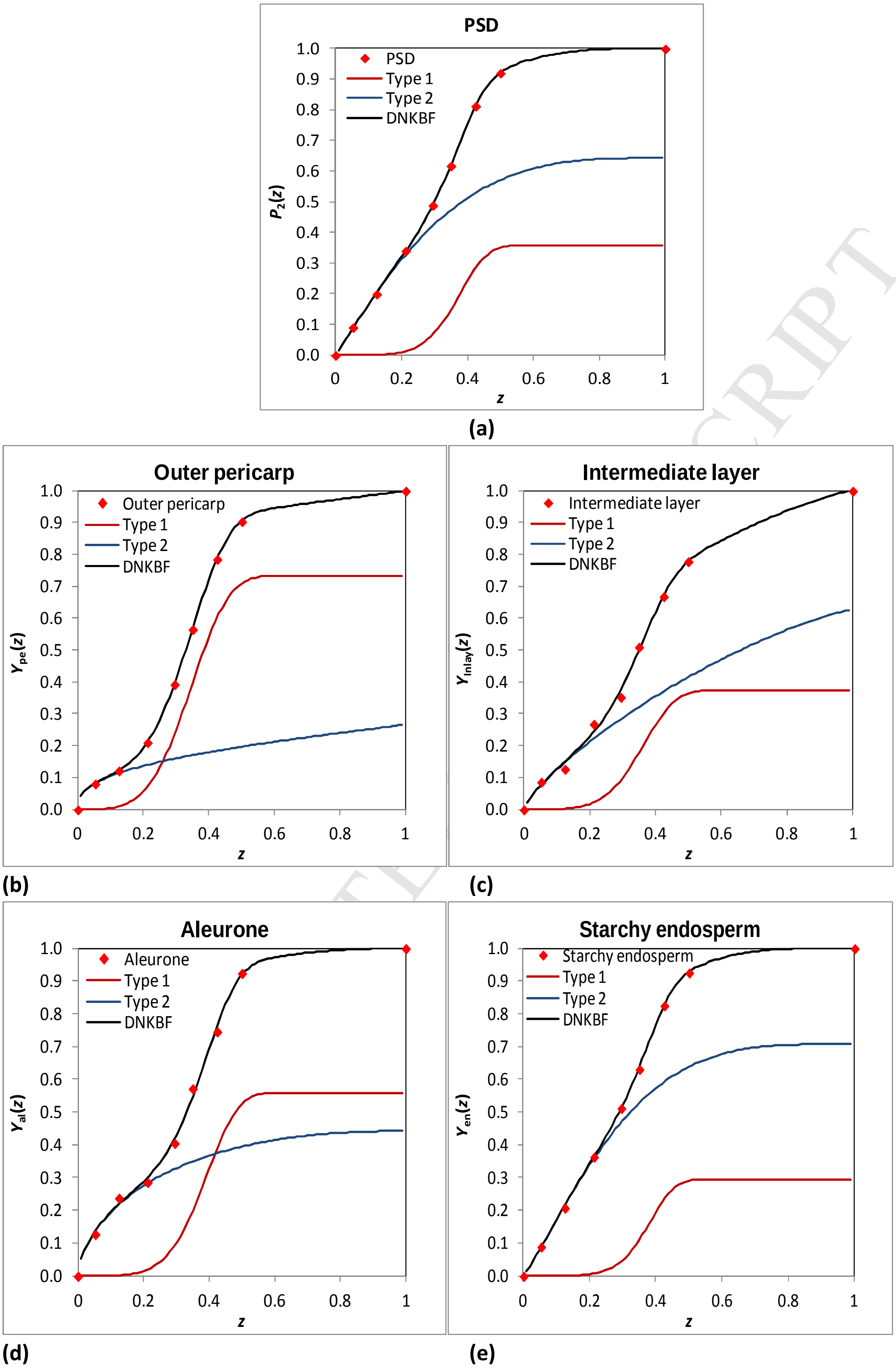

Figure 3. Cumulative particle size and component distributions, for Mallacca wheat milled under a Sharp-to-Sharp disposition.

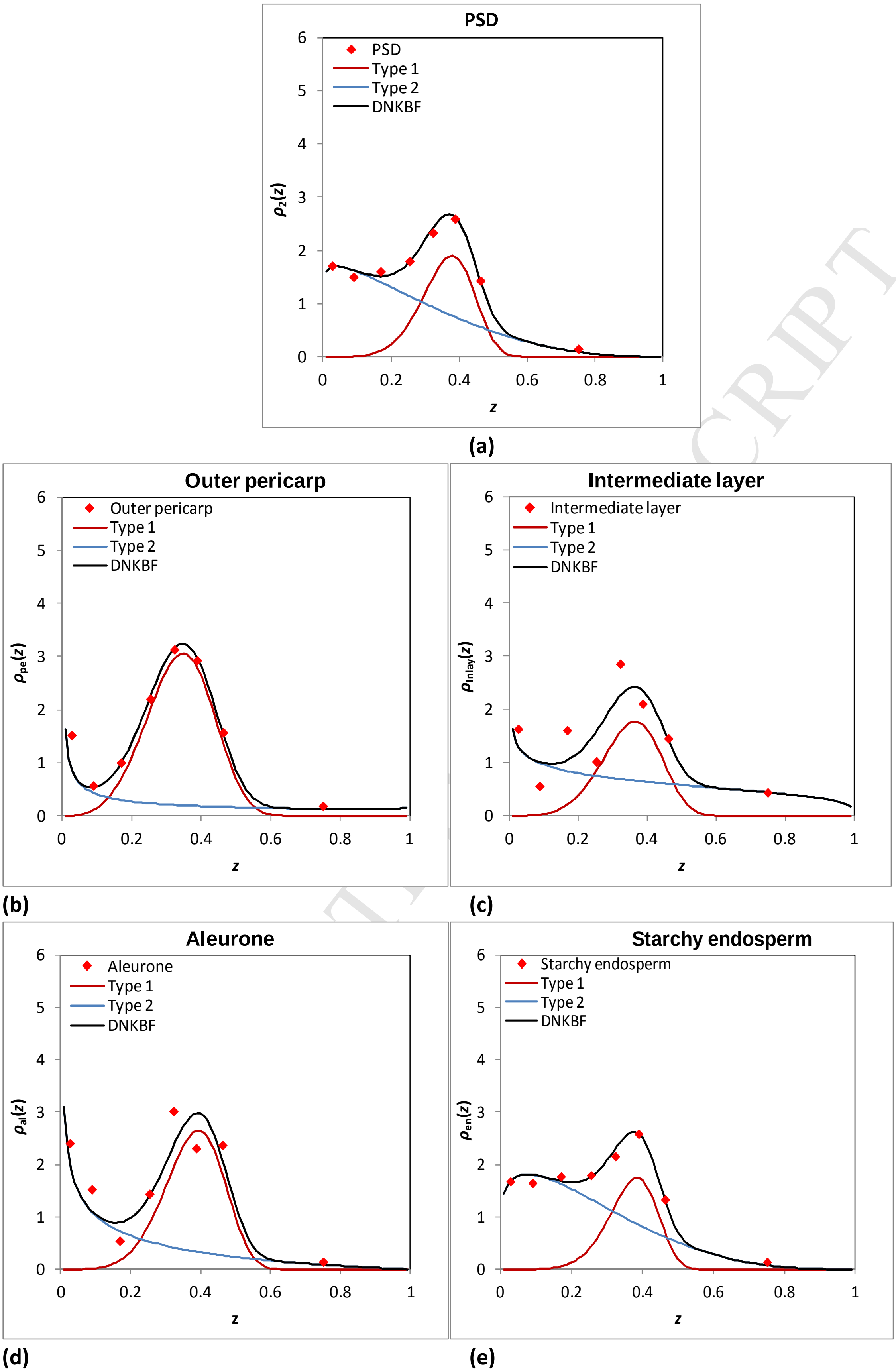

Figure 4. Non-cumulative particle size and component distributions, for Mallacca wheat milled under a Sharp-to-Sharp disposition.

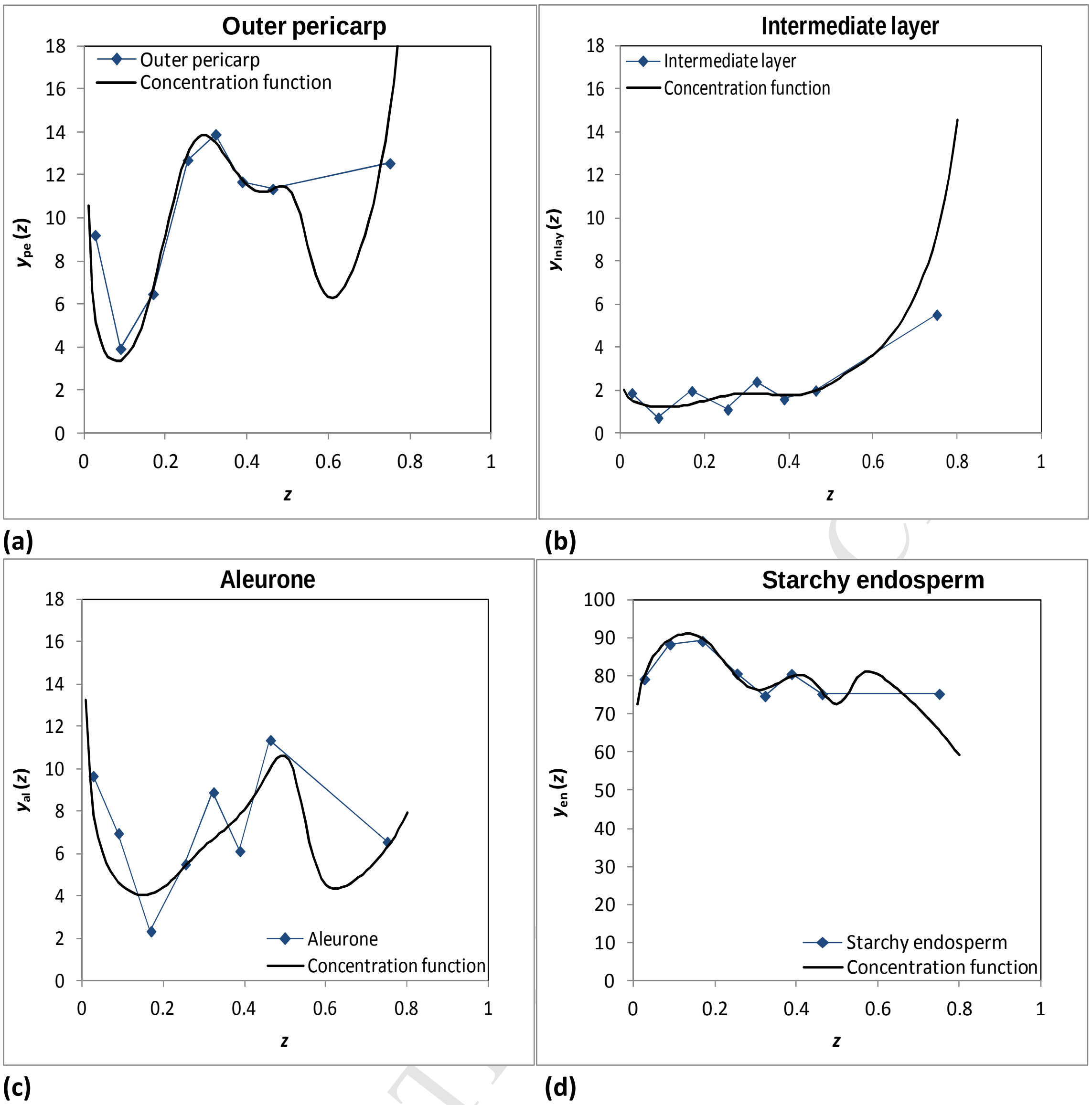

Figure 5. Concentration functions for outer pericarp, intermediate layer, aleurone and starchy endosperm, compared with experimental data, for Mallacca wheat milled under Sharp-to-Sharp disposition.

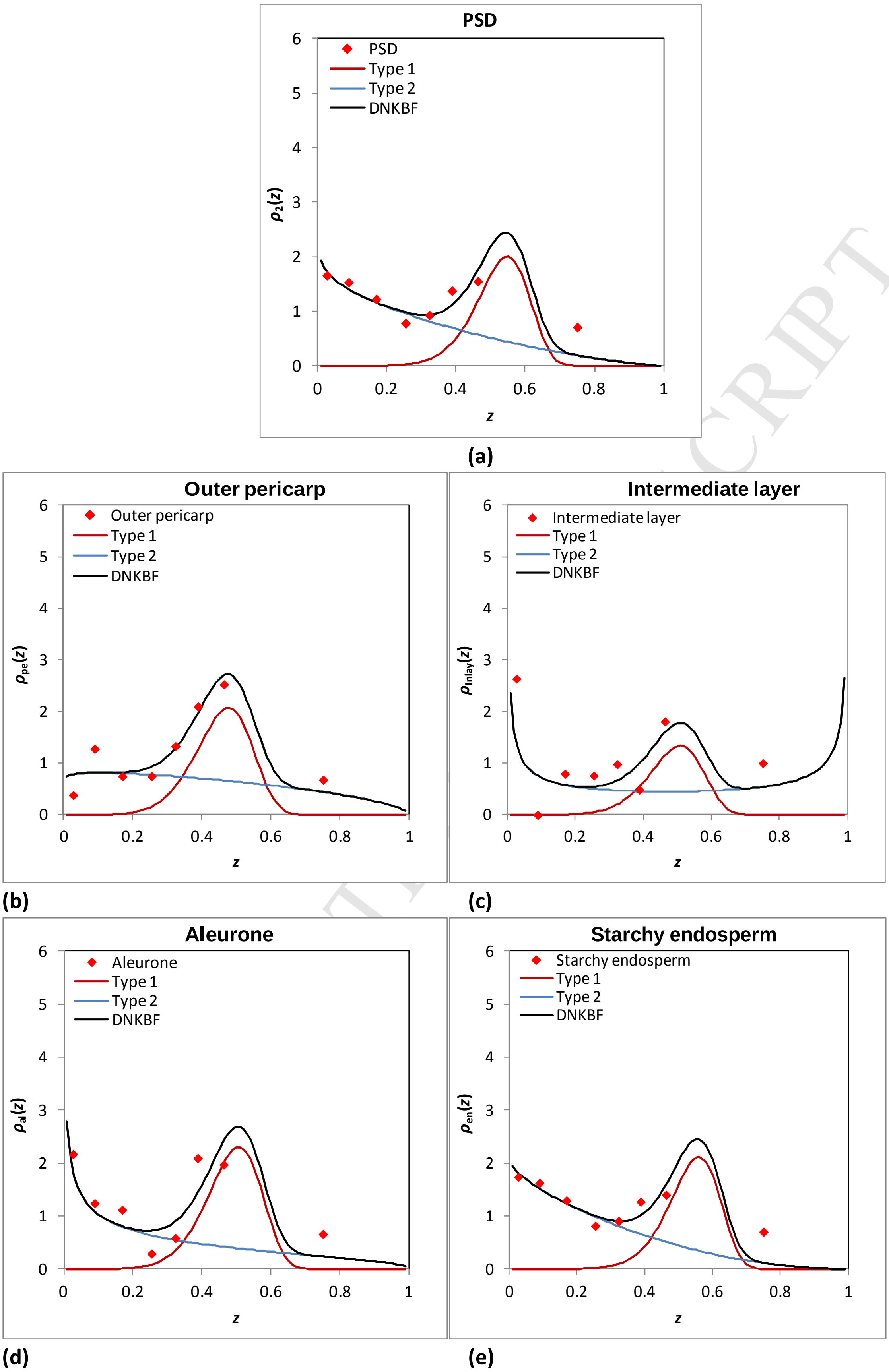

Figure 6. Non-cumulative particle size and component distributions, for Mallacca wheat milled under a Dull-to-Dull disposition.

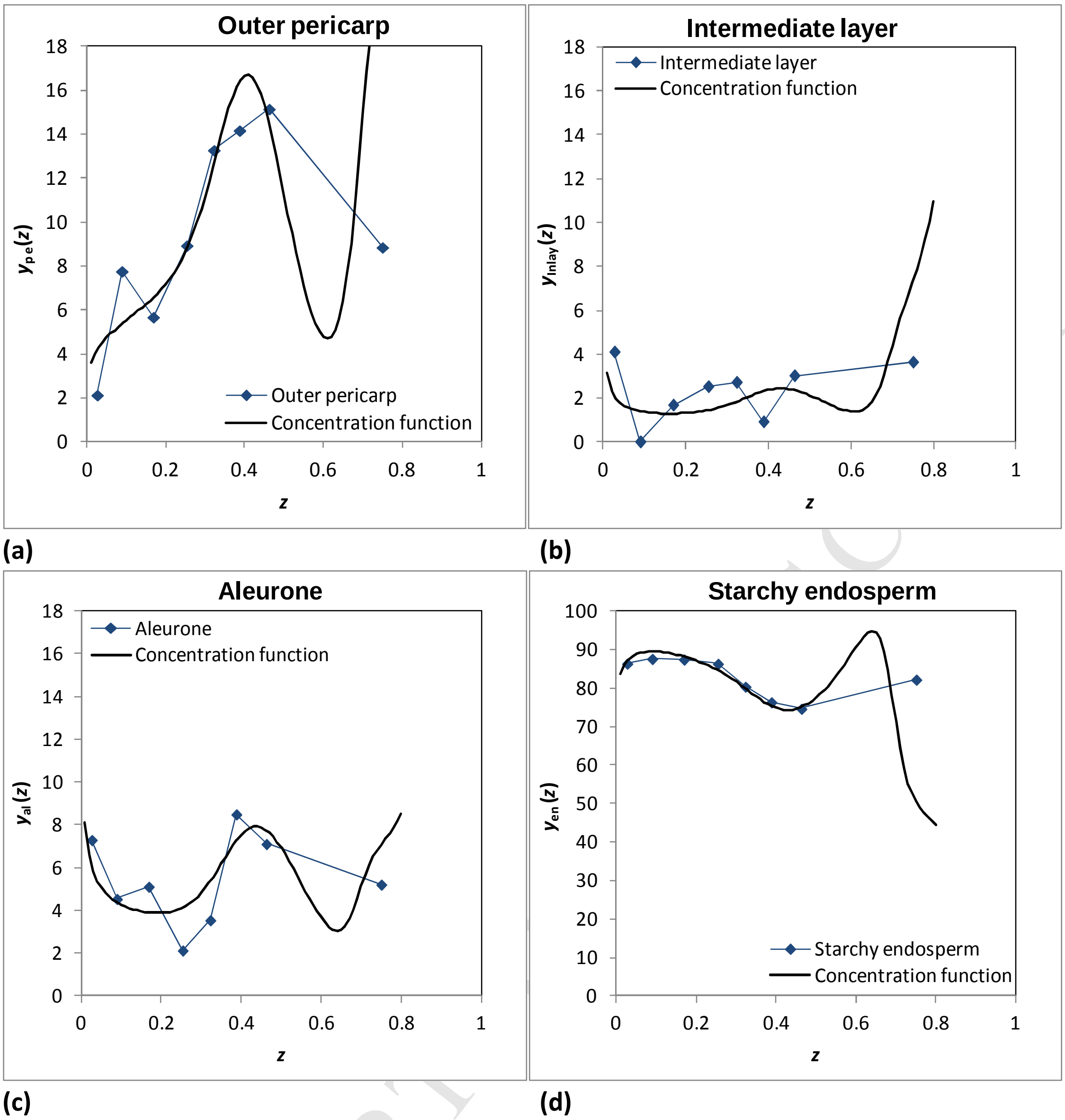

Figure 7. Concentration functions for outer pericarp, aleurone, endosperm and intermediate layer, compared with experimental data, for Mallacca wheat milled under a Dull-to-Dull disposition.

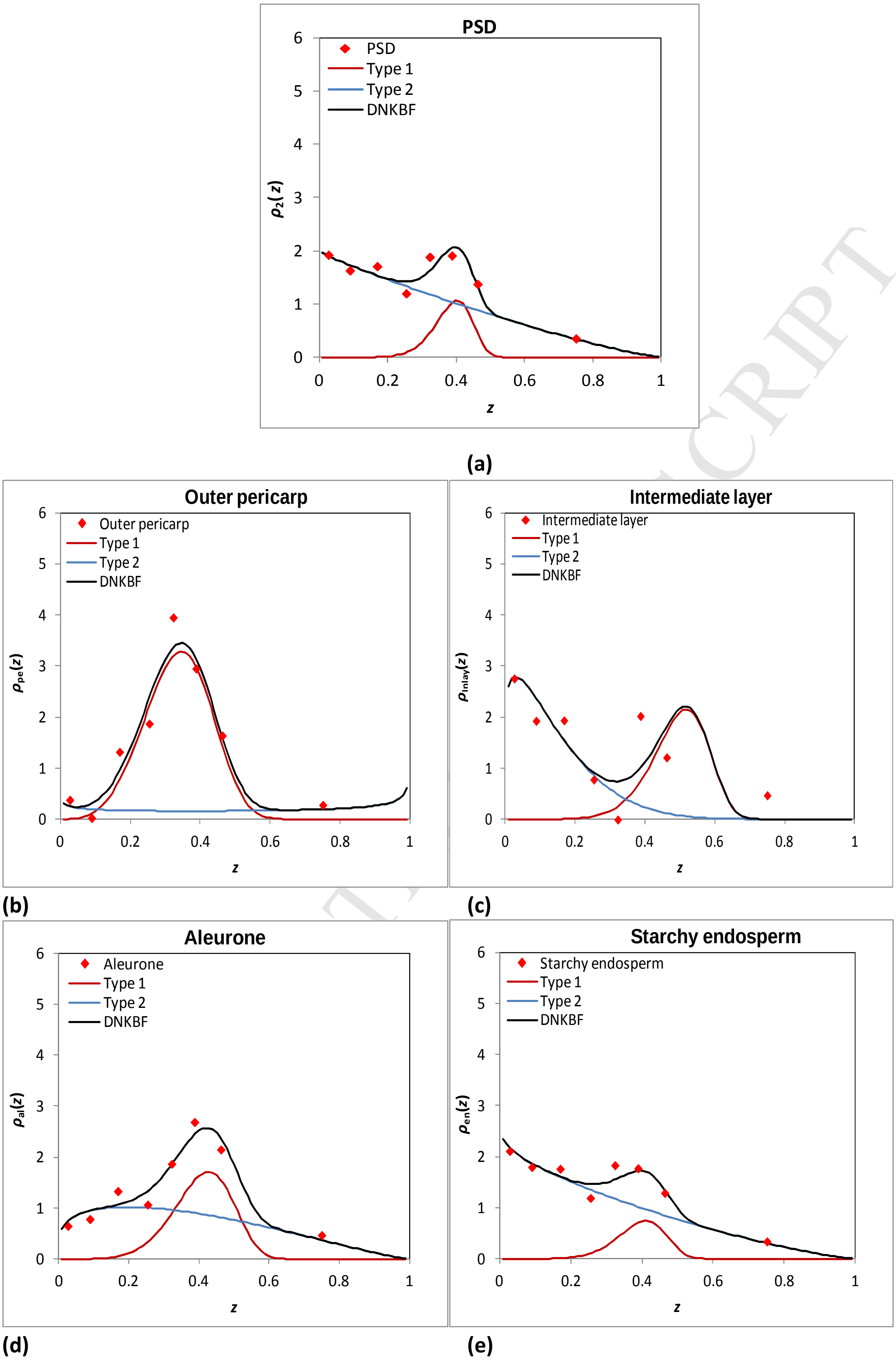

Figure 8. Non-cumulative particle size and component distributions, for Consort wheat milled under a Sharp-to-Sharp disposition.

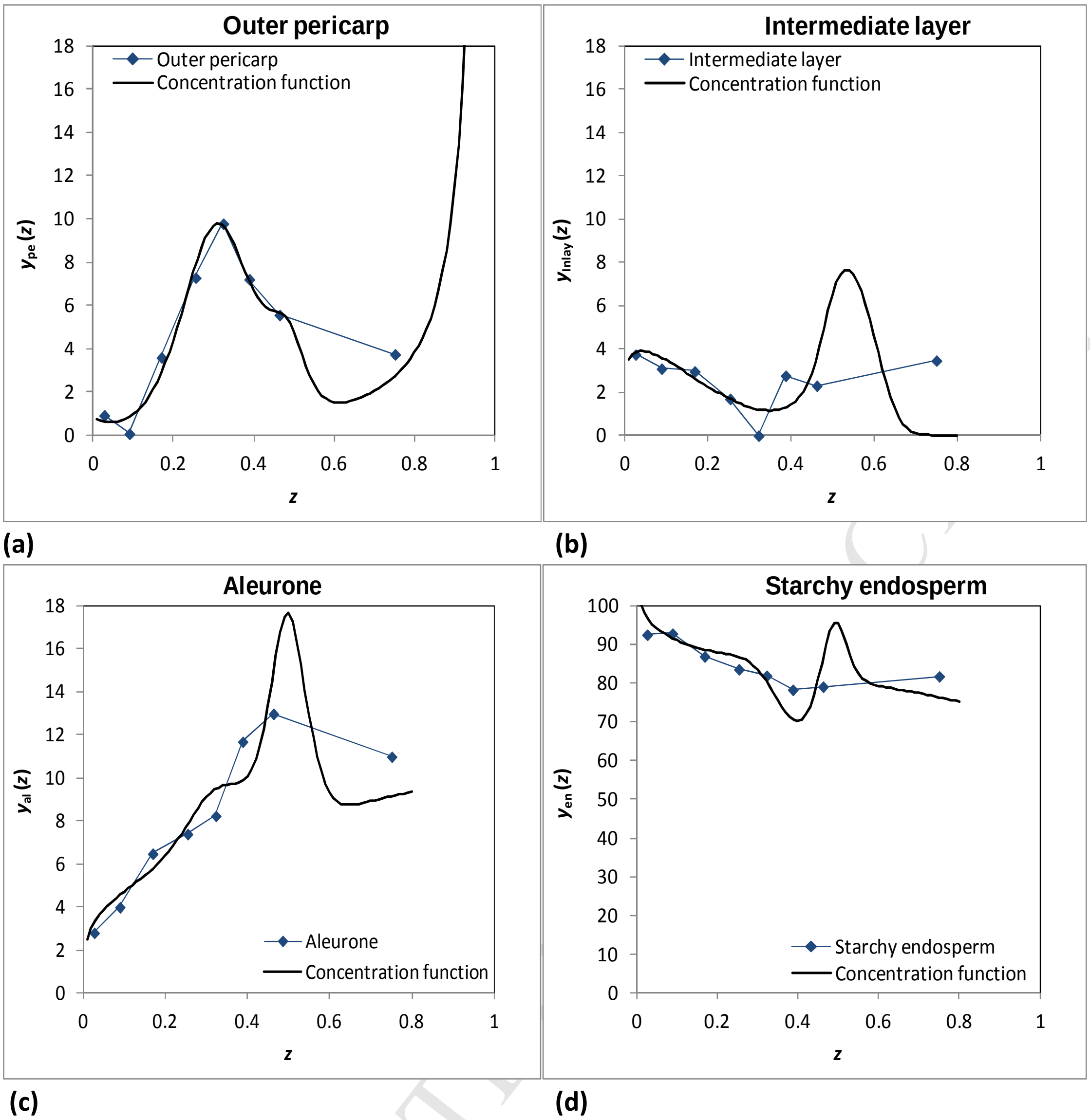

Figure 9. Concentration functions for outer pericarp, intermediate layer, aleurone and starchy endosperm, compared with experimental data, for Consort wheat milled under a Sharp-to-Sharp disposition.

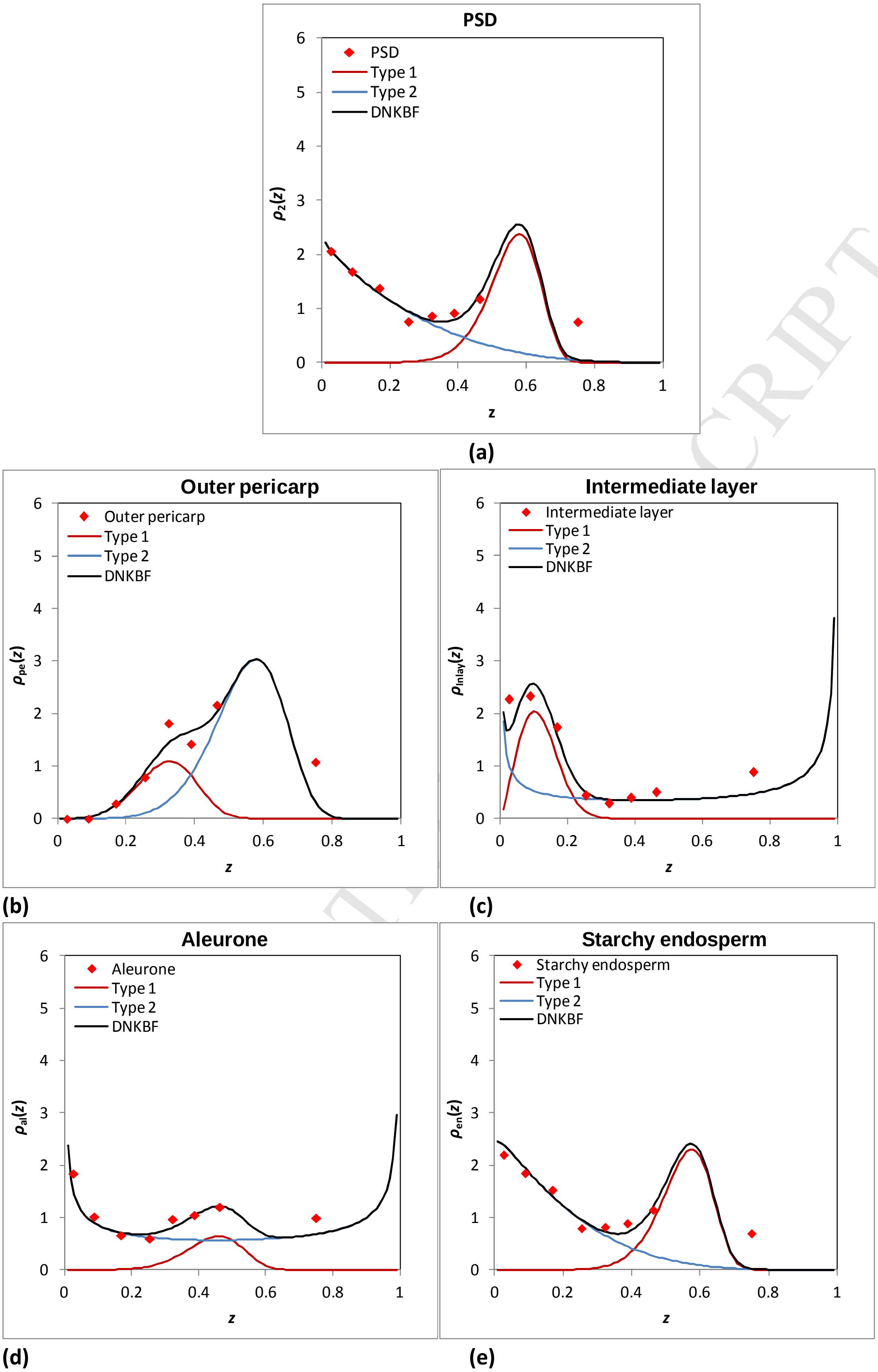

Figure 10. Non-cumulative particle size and component distributions, for Consort wheat milled under a Dull-to-Dull distribution.

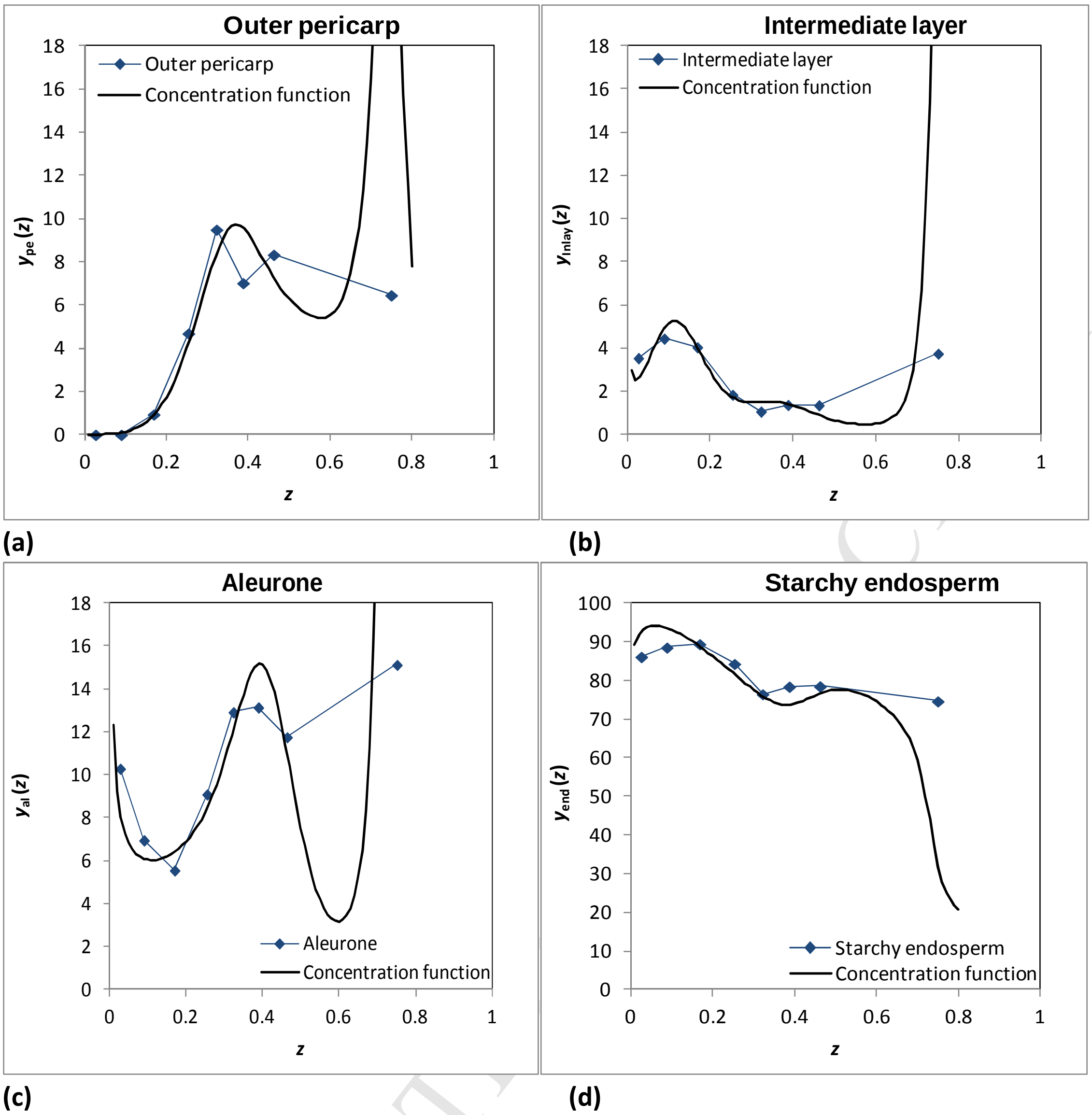

Figure 11. Concentration functions for outer pericarp, aleurone, endosperm and intermediate layer, compared with experimental data, for Consort wheat milled under a Dull-to-Dull disposition.

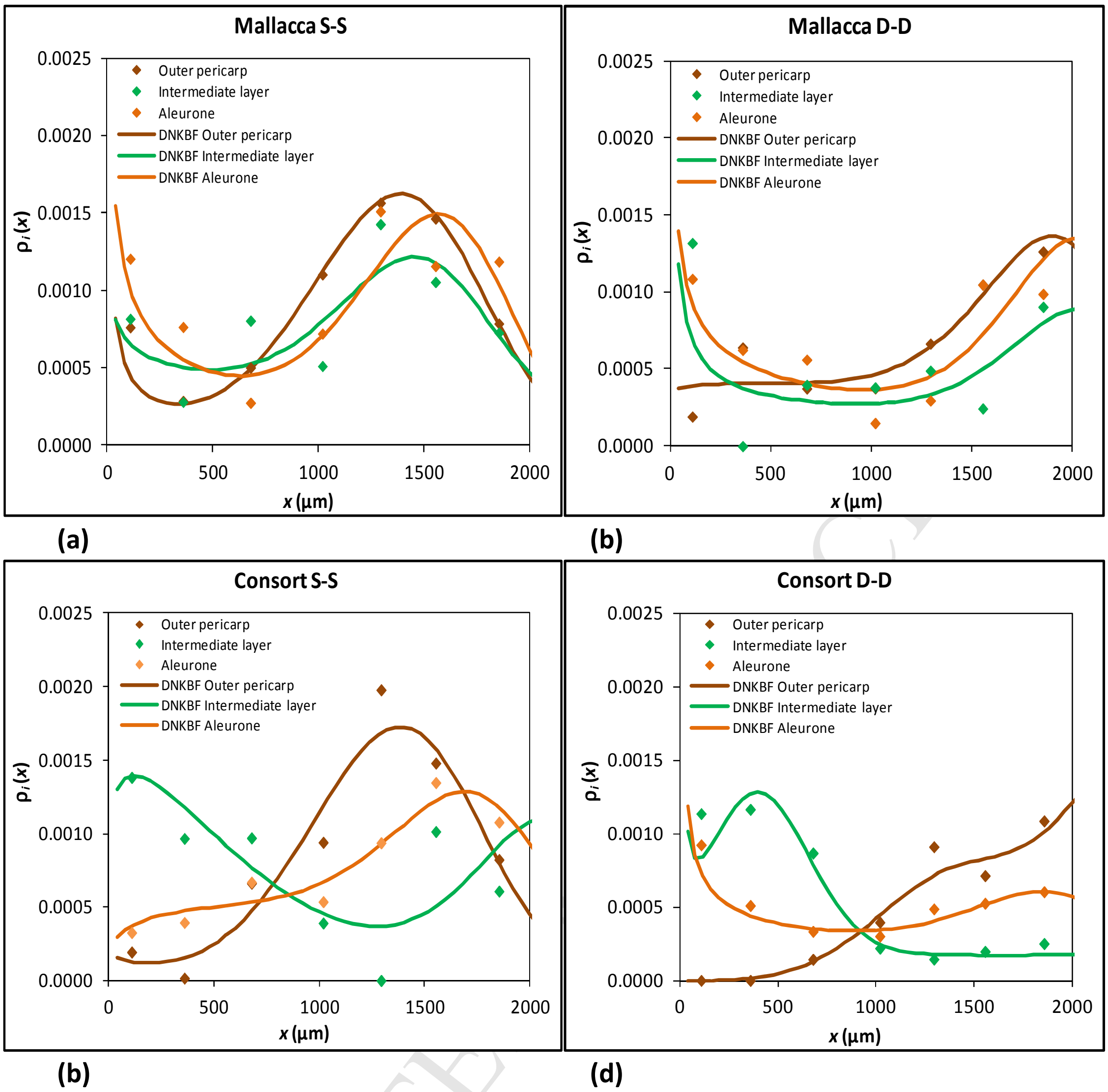

Figure 12. Outer pericarp, intermediate layer and aleurone distributions for Mallacca (a,b) and Consort (c,d) wheats milled under a Sharp-to-Sharp (a,c) and Dull-to-Dull (b,d) dispositions.

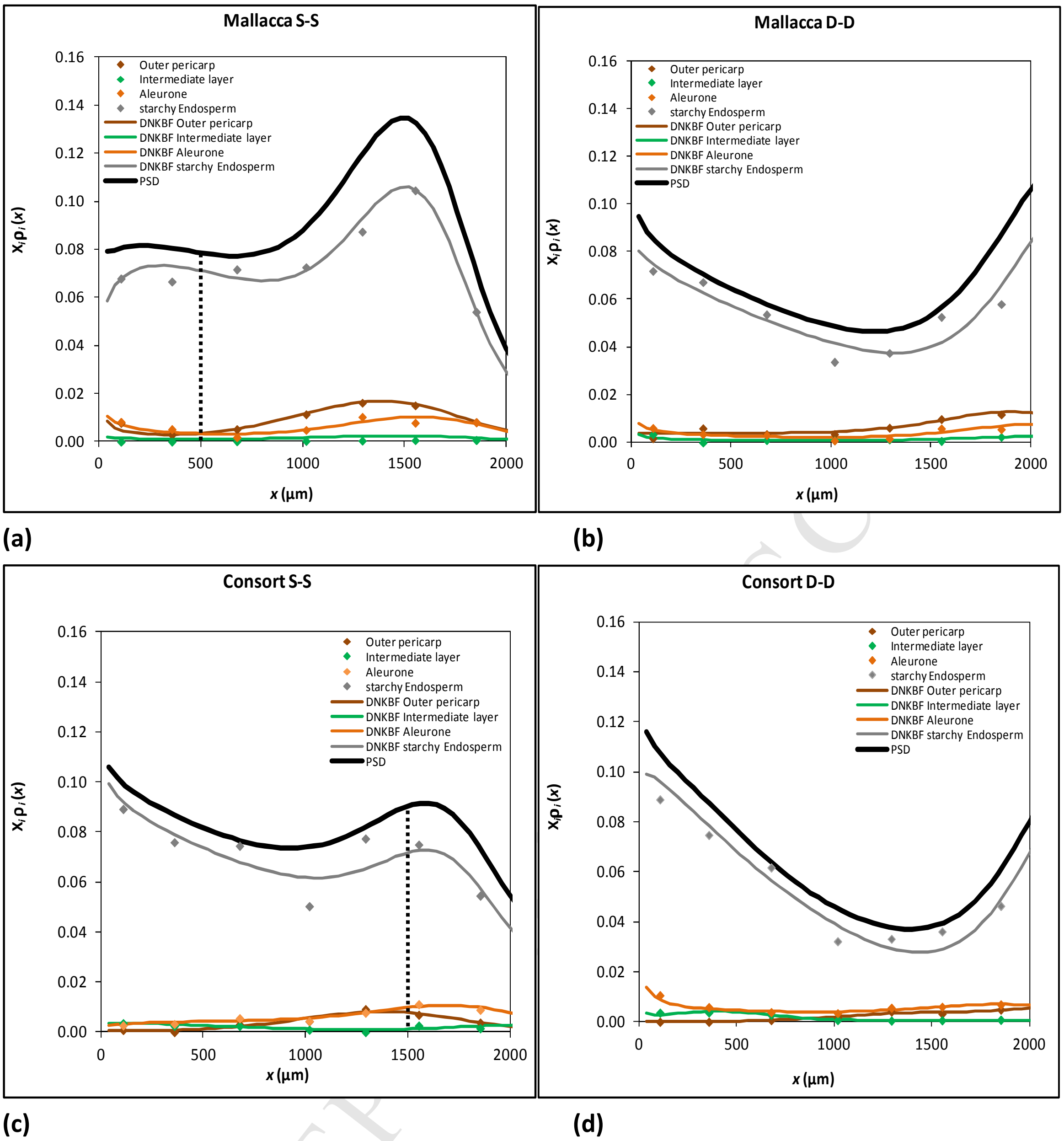

Figure 13. Outer pericarp, intermediate layer, aleurone and starchy endosperm distributions for Mallacca (a,b) and Consort (c,d) wheats milled under (a,c) Sharp-to-Sharp (a,c), and Dull-to-Dull (b,d) dispositions.

Highlights

The breakage equation for roller milling of wheat was extended to include composition

Compositional breakage functions were formulated based on spectroscopic models

Composition modelled in terms of Pericarp, Intermediate Layer, Aleurone and Endosperm

In a hard wheat these layers tended to break together, but separately in a soft wheat